

Reconciling B -decay anomalies with neutrino masses, dark matter and constraints from flavour violation

Chandan Hati ^a, Girish Kumar ^b, Jean Orloff ^a and Ana M. Teixeira ^a

^a Laboratoire de Physique de Clermont, CNRS/IN2P3 – UMR 6533, Campus des Cézeaux, 4 avenue Blaise Pascal, F-63178 Aubière Cedex, France

^b Department of Theoretical Physics, Tata Institute of Fundamental Research, Mumbai 400005, India

Abstract

Motivated by an explanation of the $R_{K^{(*)}}$ anomalies, we propose a Standard Model extension via two scalar $SU(2)_L$ triplet leptoquarks and three generations of triplet Majorana fermions. The gauge group is reinforced by a Z_2 symmetry, ensuring the stability of the lightest Z_2 -odd particle, which is a potentially viable dark matter candidate. Neutrino mass generation occurs radiatively (at the three-loop level), and leads to important constraints on the leptoquark couplings to leptons. We consider very generic textures for the flavour structure of the h_1 leptoquark Yukawa couplings, identifying classes of textures which succeed in saturating the $R_{K^{(*)}}$ anomalies. We subsequently carry a comprehensive analysis of the model's contributions to numerous high-intensity observables such as meson oscillations and decays, as well as charged lepton flavour violating processes, which put severe constraints on the flavour structure of these leptoquark extensions. Our findings suggest that the most constraining observables are $K^+ \rightarrow \pi^+ \nu \bar{\nu}$ decays, and charged lepton flavour violating $\mu - e$ conversion in nuclei (among others). Nevertheless, for several classes of flavour textures and for wide mass regimes of the new mediators (within collider reach), this Standard Model extension successfully addresses neutrino mass generation, explains the current $R_{K^{(*)}}$ tensions, and offers a viable dark matter candidate.

1 Introduction

Despite the many successes of the Standard Model (SM) in interpreting experimental data and predicting new phenomena, three independent observations signal the need to consider New Physics (NP) scenarios: neutrino oscillations, the baryon asymmetry of the Universe (BAU), and the lack of a viable dark matter (DM) candidate. Although no direct evidence for NP states has been unveiled at the LHC, certain experimental measurements have revealed non-negligible tensions with respect to the SM predictions. In addition to the anomalous magnetic moment of the muon, recent data hints to several discrepancies with respect to the SM in some B -meson decay modes, potentially suggesting the violation of lepton flavour universality (LFUV). In the SM's original formulation, gauge interactions (both charged and neutral currents) are strictly lepton flavour universal; precise measurements of related electroweak observables - for instance $Z \rightarrow \ell\ell$ decays [1] - have so far been in agreement with the SM's predictions.

The so-called $R_{K^{(*)}}$ observables are built from the comparison of the branching ratios (BR) of B into di-muon and di-electron plus $K^{(*)}$ final states, and are parametrised as

$$R_{K^{(*)}} = \frac{\text{BR}(B \rightarrow K^{(*)} \mu^+ \mu^-)}{\text{BR}(B \rightarrow K^{(*)} e^+ e^-)}. \quad (1)$$

In the above ratio of BRs, the hadronic uncertainties cancel out to a very good approximation, and consequently these observables are sensitive probes of NP contributions [2]. First results on the measurement of R_K by LHCb were reported in 2014 [3],

$$R_{K[1,6]}^{\text{LHCb}} = 0.745 \pm_{0.074}^{0.090} \pm 0.036, \quad (2)$$

having been obtained (as denoted in subscript) for the dilepton invariant mass squared bin $q^2 \in [1, 6] \text{ GeV}^2$. This corresponds to a 2.6σ deviation from the SM prediction of $R_K^{\text{SM}} = 1.00 \pm 0.01$ [4,5]. The corresponding measurements for the decays into $K^* \ell\ell$ were reported in 2017 [6],

$$R_{K^*[0.045,1.1]} = 0.66_{-0.07}^{+0.11} \pm 0.03, \quad R_{K^*[1.1,6]} = 0.69_{-0.07}^{+0.11} \pm 0.05, \quad (3)$$

respectively corresponding to 2.3σ and 2.6σ deviations from the expected SM values, $R_{K^*[0.045,1.1]}^{\text{SM}} \sim 0.92 \pm 0.02$ and $R_{K^*[1.1,6]}^{\text{SM}} \sim 1.00 \pm 0.01$ [4,5].

Interestingly, deviations from SM expectations have also been observed in $B \rightarrow D^{(*)} \ell \bar{\nu}$ decays, in particular in the ratio of tau to final states composed of light leptons,

$$R_{D^{(*)}} = \frac{\Gamma(B \rightarrow D^{(*)} \tau^- \bar{\nu})}{\Gamma(B \rightarrow D^{(*)} \ell^- \bar{\nu})} \quad (\ell = e, \mu). \quad (4)$$

The measured value for $R_D = 0.407 \pm 0.039 \pm 0.024$ [7], reported by several experiments [8–14], already deviates from the SM prediction $R_D^{\text{SM}} = 0.299 \pm 0.003$ [15] by about 2.3σ . The experimental value of $R_{D^*} = 0.304 \pm 0.013 \pm 0.007$ [7, 13, 14, 16] is also larger than the SM expectation ($R_{D^*}^{\text{SM}} = 0.260 \pm 0.008$ [17]), exhibiting a $2/6\sigma$ deviation. When combined, the latter experimental results point towards a deviation of 4.1σ from the SM prediction [7, 16, 18, 19]. Other anomalies in B meson decays have emerged concerning the angular observable P'_5 in $B \rightarrow K^* \ell^+ \ell^-$ processes. While LHCb's results for P'_5 in $B \rightarrow K^* \mu^+ \mu^-$ decays manifest a slight discrepancy with respect to the SM (either due to NP contributions, or possibly a result of SM QCD effects [20]), the Belle Collaboration [21] reported that when compared to the muon case, P'_5 results for electrons show a better agreement with respect to the SM prediction. The P'_5 results could thus be interpreted as suggestive of the fact that NP effects may be dominant for the second generation of leptons.

In view of the above tensions, numerous well-motivated beyond the SM (BSM) scenarios have been proposed in order to address one (or more) of these anomalies. Many NP models in which LFUV effects arise at the loop level do not succeed in explaining the B meson anomalies; this has fuelled the interest to consider BSM constructions capable of inducing LFUV both at tree and loop level, as in the case of models with additional gauge bosons (Z'), SM extensions via leptoquarks and other NP models (see, for example [5, 22–31] for model independent studies, [32–40] for Z' extensions, [41–62] for leptoquark models and [63–68] for further examples).

The leptoquark hypothesis - both in its scalar and vector field realisations - has been extensively explored in recent years, as have its implications for both quark and flavour dynamics. In particular, having leptoquark couplings which are necessarily flavour non-universal in the lepton sector has multiple implications concerning lepton observables, ranging from the anomalous moment of the muon, to charged lepton flavour violating (cLFV) decays and transitions. Likewise, efforts have been made to connect the neutrino mass generation problem (itself calling upon a modified lepton sector) with an explanation of the flavour tensions via leptoquarks; many such models lead to radiative generation of the light neutrino masses ¹, for instance through mixings with the standard model Higgs boson (in SM extensions via vector leptoquarks [70]), using scalar leptoquarks and color-octet Majorana fermion [55], or calling upon a “coloured Zee-Babu model” [71, 72] (with the addition of scalar leptoquarks and diquarks), which leads to two-loop radiative neutrino mass generation [73]. Extensions of SM via both leptoquarks and additional Majorana fermions aimed at connecting B -decay anomalies to neutrino masses (radiatively generated at the three-loop level), and to a solution of the dark matter problem [74, 75], relying on the so-called “coloured KNT models” [76]. These studies also evaluated the impact of the BSM construction to cLFV decays, focusing on the rôle of radiative charged lepton decays, $\ell \rightarrow \ell' \gamma$.

Building upon the previous analysis, in this work we consider a scalar leptoquark model, which aims at simultaneously explaining the B meson decay anomalies, accounting for neutrino oscillation data and putting forward a viable dark matter candidate. The SM is extended via two scalar leptoquarks $h_{1,2}$ and three generations of triplet neutrinos Σ_R^i . The SM symmetry group is enlarged by a discrete Z_2 symmetry under which only h_2 and Σ_R^i are odd. While effectively forbidding the realisation of a tree-level type III seesaw [77], the Z_2 symmetry is instrumental to ensure the stability of the lightest Z_2 -odd particle (the neutral component of the lightest triplet), which is found to be a viable dark matter candidate. Neutrino masses can be radiatively generated and, as we argue here, complying with oscillation data turns out to severely constrain the leptoquark Yukawa couplings. Focusing on saturating the $R_{K^{(*)}}$ anomalies, we carry a thorough analysis of this phenomenological model. Our study relies in assuming generic perturbative textures for the leptoquark Yukawa couplings: in particular, and contrary to previous analyses, we do not forbid couplings of the leptoquarks to the first generation of quark and leptons. Moreover we take into account a comprehensive set of flavour observables (meson and lepton rare decays and transitions); this allows to identify several classes of textures for the leptoquark Yukawa couplings in agreement with observation. Our findings suggest that the most severe constraints arise from $K \rightarrow \pi \nu \bar{\nu}$ decays and neutrinoless $\mu - e$ conversion in nuclei - and not from radiative muon decays, as suggested by other studies; furthermore, the joint interplay of these high-intensity observables also disfavors several ansätze for the leptoquark textures previously considered (see [74, 75]).

The paper is organised as follows: after presenting the building blocks of the model in Section 2, and discussing neutrino mass generation in Section 3, Section 4 is devoted to establishing first constraints on the model from the requirement of having a viable DM candidate. The B meson anomalies are presented in Section 5, and the discrepancy between SM prediction and observation

¹For a recent review of radiative neutrino mass models see for example [69].

is parametrised in terms of the leptoquark couplings. Sections 6 and 7 are dedicated to the constraints potentially arising from rare meson processes and from cLFV decays. Finally, our results (both in what concerns identifying viable textures for the leptoquark Yukawa couplings, as well as numerical studies of the model's parameter space) are collected in Section 8. We summarise the most important points, as well as our final remarks, in the Conclusions.

2 SM extensions via scalar leptoquarks and Majorana triplets

In this analysis we consider a SM extension in which two scalar leptoquarks $h_{1,2}$ and three generations of Majorana triplets Σ_R^i are introduced, respectively with $SU(3)_C \times SU(2)_L \times U(1)_Y$ charge assignments of $(\bar{\mathbf{3}}, \mathbf{3}, -1/3)$ and $(\mathbf{1}, \mathbf{3}, 0)$.

As highlighted in the Introduction, the primary goals of this model are to simultaneously address the problem of neutrino mass generation, and provide a viable DM candidate, while explaining the observed anomalies in B meson decays. If sufficiently long-lived or stable, the neutral component of the lightest triplet Σ_R^1 gives a potential cold dark matter (CDM) candidate: the quantum corrections generate a mass splitting such that the neutral component is indeed the lightest one; its stability can be ensured by reinforcing the SM gauge group by a discrete Z_2 symmetry under which both h_2 and Σ_R^i are odd, while all the SM fields and h_1 are even. Since - and as mentioned before - Σ_R^1 is the lightest state, the final DM relic abundance is solely governed by the relevant electroweak (EW) gauge interactions and $m_{\Sigma_R^1}$, independent of its Yukawa interactions. This is in contrast with scenarios in which a $SU(2)_L$ singlet fermion is considered as a dark matter candidate, subject only to Yukawa interactions.

It is important to notice that a consequence of the Z_2 symmetry is that it forbids a conventional type III seesaw mechanism; however, neutrino masses can still be radiatively generated at higher orders (as discussed in the following section), from diagrams involving the new exotic states and down-type quarks.

The complete particle spectrum is presented in Table 1.

	Field	$SU(3)_C \times SU(2)_L \times U(1)_Y$	Z_2
Fermions	$Q_L \equiv (u, d)_L^T$	$(\mathbf{3}, \mathbf{2}, 1/6)$	1
	u_R	$(\mathbf{3}, \mathbf{1}, 2/3)$	1
	d_R	$(\mathbf{3}, \mathbf{1}, -1/3)$	1
	$\ell_L \equiv (\nu, e)_L^T$	$(\mathbf{1}, \mathbf{2}, -1/2)$	1
	e_R	$(\mathbf{1}, \mathbf{1}, -1)$	1
	Σ_R	$(\mathbf{1}, \mathbf{3}, 0)$	-1
Scalars	H	$(\mathbf{1}, \mathbf{2}, 1/2)$	1
	h_1	$(\bar{\mathbf{3}}, \mathbf{3}, -1/3)$	1
	h_2	$(\bar{\mathbf{3}}, \mathbf{3}, -1/3)$	-1

Table 1: Particle content and associated charges under the SM gauge group and additional discrete symmetries.

The Lagrangian of the present SM extension can be cast as

$$\mathcal{L} = \mathcal{L}_{\text{int}}^{\text{SM}} + \mathcal{L}_{\text{int}}^{h,\Sigma} + \mathcal{L}_{\text{mass}}^{\Sigma} - V_{\text{scalar}}^{H,h}, \quad (5)$$

in which $\mathcal{L}_{\text{int}}^{h,\Sigma}$ and $V_{\text{scalar}}^{H,h}$ respectively denote the interactions of h_1, h_2 and Σ_R^i with matter², and the scalar potential, while $\mathcal{L}_{\text{mass}}^\Sigma$ encodes the Majorana mass term for the fermion triplets. The new interaction and Majorana mass terms are given by

$$\mathcal{L}_{\text{int}}^{h,\Sigma} = y_{ij} \bar{Q}_L^{C i} \epsilon(\vec{\tau} \cdot \vec{h}_1) L_L^j + z_{ij} \bar{Q}_L^{C i} \epsilon(\vec{\tau} \cdot \vec{h}_1)^\dagger Q_L^j + \tilde{y}_{ij} \overline{(\vec{\tau} \cdot \vec{\Sigma})}_R^{C i, ab} [\epsilon(\vec{\tau} \cdot \vec{h}_2) \epsilon^T]^{ba} d_R^j + \text{H.c.}, \quad (6)$$

$$\mathcal{L}_{\text{mass}}^\Sigma = -\frac{1}{2} \overline{\Sigma}^{C i} M_{ij}^\Sigma \Sigma^j. \quad (7)$$

In the above $i, j = 1 \dots 3$ denote generation indices, while $a, b = 1, 2$ are SU(2) indices; τ^c are the Pauli matrices ($c = 1, 2, 3$), and we have further defined $\epsilon^{ab} = (i\tau^2)^{ab}$. Finally, C denotes charge conjugation. The scalar potential (including SM terms) can be written as

$$\begin{aligned} V(H, h_1, h_2) &= \mu_H^2 H^\dagger H + \frac{1}{2} \lambda_H |H^\dagger H|^2 + \mu_{h_1}^2 \text{Tr}[h_1^\dagger h_1] + \mu_{h_2}^2 \text{Tr}[h_2^\dagger h_2] + \\ &+ \frac{1}{8} \lambda_{h_1} [\text{Tr}(h_1^\dagger h_1)]^2 + \frac{1}{8} \lambda_{h_2} [\text{Tr}(h_2^\dagger h_2)]^2 + \frac{1}{4} \lambda'_{h_1} \text{Tr}[(h_1^\dagger h_1)]^2 + \frac{1}{4} \lambda'_{h_2} \text{Tr}[(h_2^\dagger h_2)]^2 + \\ &+ \frac{1}{2} \lambda_{Hh_1} (H^\dagger H) \text{Tr}[h_1^\dagger h_1] + \frac{1}{2} \lambda'_{Hh_1} \sum_{i=1}^3 (H^\dagger \tau_i H) \text{Tr}[h_1^\dagger \tau_i h_1] + \\ &+ \frac{1}{2} \lambda_{Hh_2} (H^\dagger H) \text{Tr}[h_2^\dagger h_2] + \frac{1}{2} \lambda'_{Hh_2} \sum_{i=1}^3 (H^\dagger \tau_i H) \text{Tr}[h_2^\dagger \tau_i h_2] + \\ &+ \frac{1}{4} \lambda_h \text{Tr}[h_1^\dagger h_2]^2 + \frac{1}{8} \lambda'_h [\text{Tr}(h_1^\dagger h_2)]^2 + \frac{1}{4} \lambda''_h \text{Tr}[h_1^\dagger h_1] \text{Tr}[h_2^\dagger h_2] + \text{H.c.} \end{aligned} \quad (8)$$

As can be inferred from inspection of Eq. (6), the simultaneous presence of the first two terms violates baryon number, and can thus lead to $B-L$ conserving dimension-6 contributions to proton decay. In the following analysis, we will assume that these interactions are absent (i.e., $z_{ij} = 0$), an hypothesis that can naturally arise from the embedding of the model into an ultraviolet (UV) complete framework, as discussed in [79, 80]. The absence of the diquark couplings then allows to unambiguously assign baryon and lepton number to the scalar leptoquarks $h_{1,2}$.

To cast the interaction Lagrangian in a more explicit way, it is convenient to work in the $U(1)_{\text{em}}$ basis: the physical states, respectively with electric charges $4/3, -2/3, 1/3$ can be written in terms of the SU(2) components as follows

$$\begin{aligned} h_j^{4/3} &= \frac{1}{\sqrt{2}} (h_j^{(1)} - i h_j^{(2)}), \quad h_j^{-2/3} = \frac{1}{\sqrt{2}} (h_j^{(1)} + i h_j^{(2)}), \quad h_j^{1/3} = h_j^{(3)} \quad (j = 1, 2); \\ \Sigma^+ &= \frac{1}{\sqrt{2}} (\Sigma^{(1)} - i \Sigma^{(2)}), \quad \Sigma^- = \frac{1}{\sqrt{2}} (\Sigma^{(1)} + i \Sigma^{(2)}), \quad \Sigma^0 = \Sigma^{(3)} \quad (\text{for the 3 generations}). \end{aligned} \quad (9)$$

Using the above redefinitions, the interaction Lagrangian of Eq. (6) can be rewritten as

$$\begin{aligned} \mathcal{L}_{\text{int}}^{h,\Sigma} &= -y_{ij} \bar{d}_L^{C i} h_1^{1/3} \nu_L^j - \sqrt{2} y_{ij} \bar{d}_L^{C i} h_1^{4/3} e_L^j + \sqrt{2} y_{ij} \bar{u}_L^{C i} h_1^{-2/3} \nu_L^j - y_{ij} \bar{u}_L^{C i} h_1^{1/3} e_L^j \\ &- 2 \tilde{y}_{ij} \bar{\Sigma}_R^{C i} h_2^{1/3} d_R^j - 2 \tilde{y}_{ij} \bar{\Sigma}_R^{C i} h_2^{-2/3} d_R^j - 2 \tilde{y}_{ij} \bar{\Sigma}_R^{C i} h_2^{4/3} d_R^j + \text{H.c.} \end{aligned} \quad (10)$$

²The couplings of h_2 to right-handed up-type quarks are absent due to hypercharge invariance, as pointed out in [78].

Following the decomposition of Eq. (9), the most relevant interaction term for neutrino mass diagrams can now be written as

$$\frac{\lambda_h}{4} \text{Tr}(h_1^\dagger h_2 h_1^\dagger h_2) = \frac{\lambda_h}{2} h_1^{-1/3} h_2^{1/3} h_1^{-1/3} h_2^{1/3} - \lambda_h h_1^{-1/3} h_2^{-2/3} h_1^{-1/3} h_2^{4/3}. \quad (11)$$

In what follows (and for simplicity), we will further assume the couplings $\lambda'_{Hh_{1,2}}$ to be negligible; this leads to having degenerate physical masses for the components of the scalar triplets $h_{1,2}$ ($m_{h_{1(2)}}^2 = \mu_{h_{1(2)}}^2 + \lambda_{Hh_{1(2)}} v^2/2$, with v the SM Higgs vacuum expectation value), and thus allows to comply with EW precision constraints on oblique parameters.

3 Radiative neutrino mass generation and leptonic mixings

As mentioned in the previous section, the Z_2 symmetry precludes any coupling between the fermion triplets and neutral leptons, which effectively dismisses a type III seesaw explanation of neutrino mass generation (at the tree level). The absence of right-handed neutrinos further excludes the possibility of Dirac-type masses for the neutral leptons. Interestingly, the particle content of the model does allow a natural explanation to the smallness of neutrino masses: these are radiatively generated, from higher order contributions.

The first non-vanishing contributions to m_ν arise at the three-loop level, and are induced by the diagrams displayed in Fig. 1, from the exchange of leptoquarks $h_{1,2}$ and neutral (charged) fermion triplets, calling upon chirality flips in the internal down-type quark lines (proportional to the down quark masses). Despite the different particle content, the diagrams are akin to those originally proposed in [76], which were mediated via colourless scalars and a Z_2 -odd singlet Majorana fermion. (In the latter case, the computation of the contributions to m_ν has been carried in [81].)

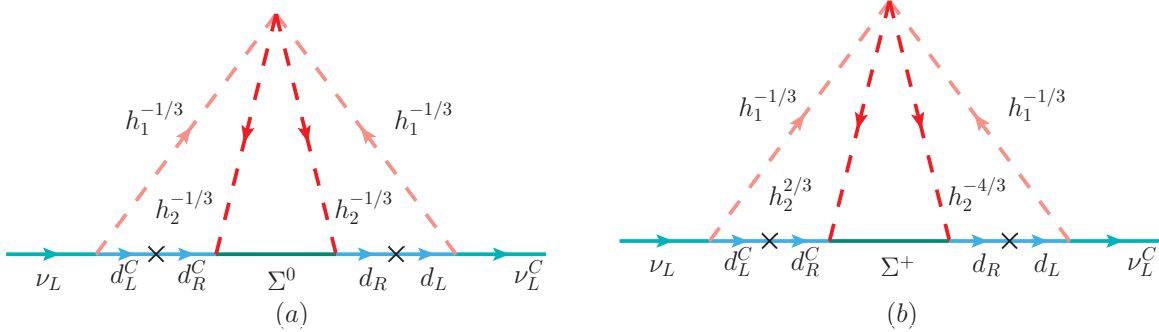


Figure 1: Three-loop diagrams contributing to neutrino masses, mediated via neutral (charged) fermion triplets. A third diagram (not displayed here) can be obtained by replacing Σ^+ by its charge conjugate state Σ^- , while also exchanging the internal $h_2^{2/3, -4/3}$ propagators of panel (b).

The computation of the different diagrams of Fig. 1 leads to the following contributions to

neutrino masses (which are for simplicity cast in the weak interaction basis):

$$\begin{aligned}
-i(m_\nu)_{\alpha\beta} = & 2 \int \frac{d^4 Q_1}{(2\pi)^4} \int \frac{d^4 Q_2}{(2\pi)^4} \frac{i}{Q_1^2 - m_{h_1}^2} (-2i y_{\alpha i}^T) P_L \frac{i}{Q_1 - m_{D_i}} \times \\
& \int \frac{d^4 k}{(2\pi)^4} (-i \tilde{y}_{ij}^T) P_L \frac{i(k + m_{\Sigma_j})}{k^2 - m_{\Sigma_j}^2} P_L (-i \tilde{y}_{jk}) \frac{i}{(k + Q_1)^2 - m_{h_2}^2} \times \\
& \left[-i(s_a \times \kappa_c) \frac{\lambda_h}{2} - 2i(s_b \times \kappa_c) \lambda_h \right] \times \\
& \frac{i}{(k - Q_2)^2 - m_{h_2}^2} \frac{i}{Q_2 - m_{D_k}} P_L (-2i y_{k\beta}) \frac{i}{Q_2^2 - m_{h_1}^2}, \tag{12}
\end{aligned}$$

in which $Q_{1,2}$ denotes the momenta of the internal down-type quarks, $m_D = \text{diag}(m_d, m_s, m_b)$ is the diagonal down-quark mass matrix³, and $P_{L,R} = (1 \mp \gamma_5)/2$. For clarity, we have explicitly highlighted the contributions of the four-scalar leptoquark vertices of diagrams (a) and (b) (as well as the Σ^- counterpart of (b)), writing them as products of symmetry and colour factors, respectively s and κ_c . Diagram (a) is associated with $s_a = 4$, while (b)-like diagrams lead to $s_b = 2$; for the colour factor one has $\kappa_c = 15$, due to the possible distinct contractions of the four-scalar leptoquark vertex (in agreement with [75]).

Using the appropriate loop integrals⁴, and after a Wick rotation we obtain

$$(m_\nu)_{\alpha\beta} = -30 \frac{\lambda_h}{(4\pi^2)^3 m_{h_2}} y_{\alpha i}^T m_{D_i} \tilde{y}_{ij}^T G \left(\frac{m_{\Sigma_j}^2}{m_{h_2}^2}, \frac{m_{h_1}^2}{m_{h_2}^2} \right) \tilde{y}_{jk} m_{D_k} y_{k\beta}, \tag{15}$$

where m_D is again the diagonal down type mass matrix (in the computation of the loop integrals, the down-quark masses are neglected when compared to the heavier $h_{1,2}$ and Σ masses in the loop), and we recall that y (\tilde{y}) denotes the Yukawa couplings of the Z_2 -even leptoquark h_1 to matter (Z_2 -odd leptoquark h_2 and triplet fermion Σ_R to down quarks); finally $G(a, b)$ is defined as

$$G(a, b) = \frac{\sqrt{a}}{8b^2} \int_0^\infty dr \frac{r}{r+a} \left[\int_0^1 dx \ln \left(\frac{x(1-x)r + (1-x)b + x}{x(1-x)r + x} \right) \right]^2, \tag{16}$$

and in the case in which (for simplicity and without loss of generality) m_Σ is assumed to be diagonal, $G(m_{\Sigma_j}^2/m_{h_2}^2, m_{h_1}^2/m_{h_2}^2)$ will also be diagonal.

The neutrino mass eigenstates can be obtained using the transformation

$$m_\nu^{\text{diag}} \equiv \text{diag}(m_{\nu_1}, m_{\nu_2}, m_{\nu_3}) = U_{i\alpha}^T (m_\nu)_{\alpha\beta} U_{\beta i}, \tag{17}$$

³For convenience, and without loss of generality, we chose to work in a basis in which the down-quark Yukawa couplings are taken to be diagonal ($Y_{ij}^d \delta_{ij} = m_{D_i}/v$), while parametrising the up-quark Yukawa couplings as $Y_{ij}^u = V_{ij}^\dagger m_{U_j}/v$, with V the Cabibbo-Kobayashi-Maskawa (CKM) mixing matrix.

⁴In particular, one makes use of the identity

$$\int \frac{d^4 Q}{(2\pi)^4} \frac{1}{(Q^2 - m_0^2)(Q^2 - m_1^2)((k+Q)^2 - m_2^2)} = i \frac{B_0(k^2, m_1^2, m_2^2) - B_0(k^2, m_0^2, m_2^2)}{16\pi^2 m_1^2}, \tag{13}$$

where B_0 is the Passarino-Veltman function defined (in terms of the renormalisation scale μ) as [82]

$$B_0(k^2, m_1^2, m_2^2) = \frac{1}{\epsilon} - \int_0^1 dx \ln \left(\frac{-x(1-x)k^2 + (1-x)m_1^2 + xm_2^2}{\mu^2} \right). \tag{14}$$

where U is the Pontecorvo-Maki-Nakagawa-Sakata (PMNS) unitary mixing matrix, which we parametrise as follows

$$U = \begin{pmatrix} c_{12}c_{13} & c_{13}s_{12} & s_{13}e^{-i\delta_D} \\ -c_{23}s_{12} - c_{12}s_{13}s_{23}e^{i\delta_D} & c_{12}c_{23} - s_{12}s_{13}s_{23}e^{i\delta_D} & c_{13}s_{23} \\ s_{12}s_{23} - c_{12}c_{23}s_{13}e^{i\delta_D} & -c_{12}s_{23} - c_{23}s_{12}s_{13}e^{i\delta_D} & c_{13}c_{23} \end{pmatrix} \cdot \text{diag}(1, e^{i\alpha/2}, e^{i\beta/2}). \quad (18)$$

In the above, $s_{ij} \equiv \sin(\theta_{ij})$ and $c_{ij} \equiv \cos(\theta_{ij})$; δ_D is the CP violating Dirac phase while α and β are Majorana phases.

It is important to notice that as can be seen from Eqs. (15) and (17), neutrino masses (and leptonic mixings) do indeed depend on both of the Yukawa couplings involving the leptoquarks, y and \tilde{y} . In particular, the former will be at the source of a number of flavour transitions, including rare meson decays, neutral meson-antimeson oscillations as well as charged lepton flavour violating processes. This implies that a strong connection between neutrino phenomena and flavour nonuniversal processes is established via the flavour structure of the Yukawa matrix y .

In the absence of a complete framework proving a full theory of flavour (which would suggest a structure for y and \tilde{y}), one can nevertheless parametrise one of the Yukawa couplings - for example, \tilde{y} - using a modified Casas-Ibarra parametrisation [83], which further allows to accommodate neutrino oscillation data.

In order to construct the modified Casas-Ibarra parametrisation, we first notice that from Eqs. (15) and (17) one can write the diagonal neutrino mass matrix as

$$m_\nu^{\text{diag}} = U^T y^T m_D \tilde{y}^T F(\lambda_h, m_\Sigma, m_{h_{1,2}}) \tilde{y} m_D y U, \quad (19)$$

in which we have omitted flavour (generation) indices for simplicity, and where

$$F(\lambda_h, m_\Sigma, m_{h_{1,2}}) = \frac{30 \lambda_h}{(4\pi^2)^3 m_{h_2}} G_j \left(\frac{m_{\Sigma_j}^2}{m_{h_2}^2}, \frac{m_{h_1}^2}{m_{h_2}^2} \right). \quad (20)$$

As noted before, for a diagonal m_Σ , G and thus F are also diagonal matrices in generation space, which allows to write the identity

$$(\sqrt{m_\nu^{\text{diag}}}^{-1} U^T y^T m_D \tilde{y}^T \sqrt{F}) (\sqrt{F} \tilde{y} m_D y U \sqrt{m_\nu^{\text{diag}}}^{-1}) = \mathbb{1} = \mathcal{R}^T \mathcal{R}, \quad (21)$$

with \mathcal{R} an arbitrary complex orthogonal matrix ($\mathcal{R}^T \mathcal{R} = \mathbb{1}$) which can be parametrised in terms of three complex angles, θ_i ($i = 1 - 3$). Finally, from Eq. (21) one obtains the modified Casas-Ibarra parametrisation, which allows to write the Yukawa couplings of the h_2 leptoquark in terms of observable quantities (light neutrino masses, leptonic mixings, down quark masses, triplet and leptoquark masses), and of two unknown quantities - the h_1 leptoquark Yukawa couplings and a complex orthogonal matrix - as

$$\tilde{y} = F^{-1/2} \mathcal{R} \sqrt{m_\nu^{\text{diag}}} U^\dagger y^{-1} m_d^{-1}. \quad (22)$$

The above parametrisation (which is in agreement to a similar approach carried in [75]), allows to write the couplings \tilde{y} in terms of y up to a complex orthogonal matrix. As will be discussed in detail in Section 8.1, once the approximate flavour texture of y is inferred from various experimental constraints, that of \tilde{y} can be derived (up to the mixings due to \mathcal{R}).

4 A viable dark matter candidate

Reinforcing the SM gauge group via a discrete Z_2 symmetry ensures the stability of the lightest state which is odd under Z_2 . If the lightest Z_2 -odd particle (LZoP) is neutral, and the strength of its interactions is such that its relic abundance is in agreement with observational data, then it can be indeed a viable dark matter candidate.

In our analysis we assume that the spectrum of the new states is such that one has $m_{\Sigma_R^1} < m_{h_2}$. At the tree level, all the components of a generation Σ_R^i have the same mass $m_{\Sigma^i, \text{tree}} = m_{\Sigma^i, \pm} = m_{\Sigma^i, 0}$. The degeneracy between the components is broken by EW radiative corrections, which render the charged states heavier than the neutral one. Dropping for simplicity the generation indices (in this section our discussion is focused on the components of the lightest triplet, Σ_R^1), the splitting between the neutral and charged components is given by [84]

$$\Delta_{m_\Sigma} = m_{\Sigma^\pm} - m_{\Sigma^0} = \frac{\alpha_2 m_\Sigma^{\text{tree}}}{4\pi} [f_{\text{EW}}(x_{W\Sigma}) - \cos^2 \theta_w f_{\text{EW}}(x_{Z\Sigma})], \quad (23)$$

with $x_{ij} = \frac{m_i}{m_j}$ and

$$f_{\text{EW}}(x) = -x^2 + x^4 \ln x + x(x^2 - 4)^{1/2} \left(1 + \frac{x^2}{2}\right) \ln \left(-1 - \frac{x}{2}(x^2 - 4)^{1/2} + \frac{x^2}{2}\right) \frac{x}{2}, \quad (24)$$

and in which $\alpha_2 = \alpha_e / \sin^2 \theta_w$, with α_e the fine structure constant and θ_w the weak mixing angle. In the limit $m_\Sigma \gg M_{W,Z}$ (justified by negative searches at LHC and EW precision measurements), the EW radiative corrections are found to be of order $m_{\Sigma^\pm} - m_{\Sigma^0} \sim 166$ MeV. While the latter mass difference is enough to ensure that the neutral component of the lightest triplet, Σ^0 , is indeed the LZoP, it is sufficiently small to be neglected in the subsequent (numerical) analysis.

The relic abundance of the LZoP Σ^0 is determined by its interactions and by the annihilation and coannihilation channels open in view of the particle mass spectrum. In addition to the Yukawa interactions with h_2 , the Σ_R triplets are subject to $\text{SU}(2)_L$ gauge interactions. Since, as previously highlighted, we assume that $m_{\Sigma_R^1} < m_{h_2}$, the relic density of Σ^0 is, to first order approximation⁵, solely determined by its gauge interactions, which govern the distinct annihilation and coannihilation channels (involving also the charged components Σ^\pm). In particular, the annihilation and coannihilation processes involve the following channels: $\Sigma^0 \Sigma^0 \rightarrow W^\pm W^\mp$ through t -channel Σ^\pm exchange; $\Sigma^0 \Sigma^\pm \rightarrow W^\pm Z^0$ via t -channel Σ^\pm exchange; $\Sigma^0 \Sigma^\pm \rightarrow W^\pm Z^0, W^\pm H, \bar{f} f'$ (via s -channel W^\pm exchange). Other processes involving the charged components of the triplet fermion must be also taken into account in the Boltzmann equations leading to the computation of the relic density. These include $\Sigma^\pm \Sigma^\mp \rightarrow Z^0 Z^0 (W^\pm W^\mp)$ through $\Sigma^{\pm(0)}$ t -channel exchange, $\Sigma^\pm \Sigma^\mp \rightarrow W^\pm W^\mp, Z^0 H, \bar{f} f$ (s -channel via Z^0 mediation), and finally $\Sigma^\pm \Sigma^\pm \rightarrow W^\pm W^\pm$ through Σ^0 exchange (t -channel).

The relevant cross sections for the above mentioned processes are given by [85]

$$\begin{aligned} \sigma(\Sigma^0 \Sigma^0)|_{\bar{v}} &\simeq 2\pi \frac{\alpha_2^2}{m_\Sigma^2}, & \sigma(\Sigma^0 \Sigma^\pm)|_{\bar{v}} &\simeq 2\pi \frac{29 \alpha_2^2}{16 m_\Sigma^2}, \\ \sigma(\Sigma^+ \Sigma^-)|_{\bar{v}} &\simeq 2\pi \frac{37 \alpha_2^2}{16 m_\Sigma^2}, & \sigma(\Sigma^\pm \Sigma^\pm)|_{\bar{v}} &\simeq 2\pi \frac{\alpha_2^2}{2 m_\Sigma^2}, \end{aligned} \quad (25)$$

⁵A full evaluation of the relic density would further call upon higher order effects, which would in turn depend on the Yukawa couplings of the LZoP, and other additional interactions. Such a study lies beyond the scope of the present analysis; here our primary goal is to identify a viable dark matter candidate, and obtain indicative constraints on its mass.

where only the coefficients a_{ij} are kept in the relative velocity (\bar{v}) expansion of the cross section, i.e. $\sigma_{ij}|\bar{v}| = a_{ij} + b_{ij}\bar{v}^2$.

The computation of the relic abundance follows closely the method of [86], in which the freeze-out temperature of the LZoP Σ^0 ($x_f \equiv m_\Sigma/T_f$) is obtained in terms of the thermally averaged effective cross section $\langle\sigma_{\text{eff}}|\bar{v}|\rangle$. The relevant channels above referred to contribute to the thermally averaged effective cross section $\langle\sigma_{\text{eff}}|\bar{v}|\rangle$ as

$$\begin{aligned} \langle\sigma_{\text{eff}}|\bar{v}|\rangle = & \frac{g_0^2}{g_{\text{eff}}^2} \sigma(\Sigma^0\Sigma^0)|\bar{v}| + 4 \frac{g_0 g_\pm}{g_{\text{eff}}^2} \sigma(\Sigma^0\Sigma^\pm)|\bar{v}| \left(1 + \frac{\Delta m_\Sigma}{m_\Sigma}\right)^{3/2} \exp\left(-\frac{\Delta m_\Sigma}{m_\Sigma} x_f\right) + \\ & + \frac{g_\pm^2}{g_{\text{eff}}^2} [2\sigma(\Sigma^+\Sigma^-)|\bar{v}| + 2\sigma(\Sigma^\pm\Sigma^\pm)|\bar{v}|] \left(1 + \frac{\Delta m_\Sigma}{m_\Sigma}\right)^3 \exp\left(-2\frac{\Delta m_\Sigma}{m_\Sigma} x_f\right), \end{aligned} \quad (26)$$

and the freeze-out temperature is then recursively given by

$$x_f \equiv \frac{m_\Sigma}{T_f} = \ln \left(\frac{0.038 g_{\text{eff}} M_{\text{Pl}} m_\Sigma \langle\sigma_{\text{eff}}|\bar{v}|\rangle}{g_*^{1/2} x_f^{1/2}} \right), \quad (27)$$

in which $g_* \sim 106.75$ is the total number of effective relativistic degrees of freedom the freeze-out, and $M_{\text{Pl}} = 1.22 \times 10^{19}$ GeV is the Planck scale. The quantity g_{eff} is related to the degrees of freedom of the triplet components, $g_0 = 2$ and $g_\pm = 2$, respectively for Σ^0 and Σ^\pm and to Δm_Σ (the mass splitting between the charged and neutral components of Σ_R), and can be written as

$$g_{\text{eff}} = g_0 + 2g_\pm \left(1 + \frac{\Delta m_\Sigma}{m_\Sigma}\right)^{3/2} \exp\left(-\frac{\Delta m_\Sigma}{m_\Sigma} x_f\right). \quad (28)$$

Finally, the relic abundance is given by

$$\Omega h^2 = \frac{1.07 \times 10^9 x_f}{g_*^{1/2} M_{\text{Pl}}(\text{GeV}) I_a}, \quad (29)$$

with I_a the annihilation integral, which is defined as

$$I_a = x_f \int_{x_f}^{\infty} x^{-2} a_{\text{eff}} dx. \quad (30)$$

In the above, one has used the approximation $a_{\text{eff}} \sim \sigma_{\text{eff}}|\bar{v}|$ (we recall that we have not taken into account the second and higher order terms in the relative velocity expansion of the effective cross section).

For our purpose of constraining the parameter space of the model, we will rely on a simple iterative solution of Eq. (29), which allows to infer first limits on the values of $m_{\Sigma_R^1}$ leading to a relic density in agreement with the most recent observational data [87],

$$\Omega h^2 = 0.1186 \pm 0.0020. \quad (31)$$

The results of this (approximative) numerical analysis are displayed in Fig. 2, which reveals that having an LZoP mass in the range $2.425 \text{ TeV} < m_\Sigma < 2.465 \text{ TeV}$ leads to a dark matter relic abundance in agreement with the latest data. In what follows, we will use $m_\Sigma \sim 2.45 \text{ TeV}$ as an illustrative benchmark value for the lightest fermion triplet mass.

Although already mentioned, we nevertheless stress again that several approximations were done in our computation of the relic abundance; moreover, one should also explicitly solve the

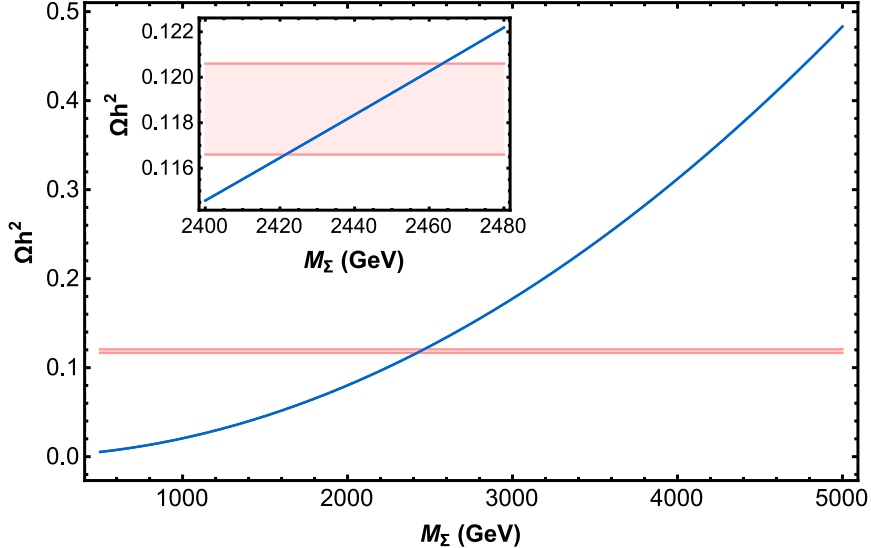


Figure 2: Estimated relic abundance (see text for details) of the dark matter candidate, Σ^0 , as a function of its mass. The rose-coloured band corresponds to the latest observational data $\Omega h^2 = 0.1198 \pm 0.0015$ [87].

coupled Boltzmann equations to numerically obtain the allowed mass range of the LZoP (the lightest Σ^0). Other than complying with the dark matter relic abundance, the potential candidate is also subject to the increasingly strong constraints from direct and indirect searches (see, e.g. [84, 88]); a detailed discussion of the latter (and the dedicated facilities) lies beyond the scope of this work.

5 Addressing the B meson decay anomalies

As can be seen from the interaction Lagrangian of Eq. (10), the scalar leptoquark h_1 couples to both down-type quarks and charged leptons, the couplings having a priori a non-trivial structure in flavour space. This will open the door to new contributions to numerous rare flavour changing transitions and decays, and - most importantly - can potentially lead to lepton flavour non-universal effects, such as those currently suggested by the reported LHCb anomalies.

In this section we will explore to which extent the current model succeeds in addressing the B meson decay anomalies, $R_{K^{(*)}}$ and $R_{D^{(*)}}$, respectively associated with neutral and charged current transitions. The abundant constraints arising from negative searches for NP effects in meson oscillation and decays, as well as in charged lepton flavour violating observables will be discussed in Sections 6 and 7.

5.1 Neutral current anomalies: R_K and R_{K^*}

As mentioned in the Introduction, recent measurements [3, 6] of the ratios of branching ratios of $B \rightarrow K(K^*)\ell\ell$ decays into pairs of muons over those into di-electrons exhibit non-negligible

deviations when compared to the SM predictions [4, 5]; as already stated one has

$$\begin{aligned}
R_{K[1,6]} &= 0.745 \pm_{0.074}^{0.090} \pm 0.036, & R_K^{\text{SM}} &= 1.00, \pm 0.01 \\
R_{K^*[0.045,1.1]} &= 0.66 \pm_{-0.07}^{+0.11} \pm 0.03, & R_{K^*}^{\text{SM}} &\sim 0.92 \pm 0.02 \\
R_{K^*[1.1,6]} &= 0.69 \pm_{-0.07}^{+0.11} \pm 0.05, & R_{K^*}^{\text{SM}} &\sim 1.00 \pm 0.01,
\end{aligned} \tag{32}$$

where the dilepton invariant mass squared bin (in GeV^2) is identified by the subscript. The comparison of SM predictions with observation respectively reveals deviations of 2.6σ , 2.4σ and 2.5σ .

For the leptoquark mass regime considered here (multi-TeV), the neutral current effects induced by the heavy degrees of freedom (SM and NP contributions) in the quark level transitions $d_j \rightarrow d_i \ell^+ \ell^-$ can be described by the following effective Hamiltonian [89, 90]

$$\begin{aligned}
\mathcal{H}(d_j \rightarrow d_i \ell^+ \ell^-) &= -\frac{4G_F}{\sqrt{2}} V_{tj} V_{ti}^* \left[C_7^{ij} \mathcal{O}_7^{ij} + C_{7'}^{ij} \mathcal{O}_{7'}^{ij} + \sum_{X=9,10,S,P} \left(C_X^{ij;\ell\ell'} \mathcal{O}_X^{ij;\ell\ell'} + C_{X'}^{ij;\ell\ell'} \mathcal{O}_{X'}^{ij;\ell\ell'} \right) \right. \\
&\quad \left. + C_T^{ij;\ell\ell'} \mathcal{O}_T^{ij;\ell\ell'} + C_{T5}^{ij;\ell\ell'} \mathcal{O}_{T5}^{ij;\ell\ell'} \right] + \text{H.c.}, \tag{33}
\end{aligned}$$

in which G_F is the Fermi constant and V is the CKM mixing matrix. The effective operators present in the above equation can be defined as (for simplicity, hereafter we drop the ij superscripts, which are set to $i, j = s, b$ for the process $b \rightarrow s \ell^+ \ell^-$):

$$\begin{aligned}
\mathcal{O}_7 &= \frac{em_{d_j}}{(4\pi)^2} (\bar{d}_i \sigma_{\mu\nu} P_R d_j) F^{\mu\nu}, \\
\mathcal{O}_9^{\ell\ell'} &= \frac{e^2}{(4\pi)^2} (\bar{d}_i \gamma^\mu P_L d_j) (\bar{\ell} \gamma_\mu \ell'), & \mathcal{O}_{10}^{\ell\ell'} &= \frac{e^2}{(4\pi)^2} (\bar{d}_i \gamma^\mu P_L d_j) (\bar{\ell} \gamma_\mu \gamma_5 \ell'), \\
\mathcal{O}_S^{\ell\ell'} &= \frac{e^2}{(4\pi)^2} (\bar{d}_i P_R d_j) (\bar{\ell} \ell'), & \mathcal{O}_P^{\ell\ell'} &= \frac{e^2}{(4\pi)^2} (\bar{d}_i P_R d_j) (\bar{\ell} \gamma_5 \ell'), \\
\mathcal{O}_T^{\ell\ell'} &= \frac{e^2}{(4\pi)^2} (\bar{d}_i \sigma_{\mu\nu} d_j) (\bar{\ell} \sigma^{\mu\nu} \ell'), & \mathcal{O}_{T5}^{\ell\ell'} &= \frac{e^2}{(4\pi)^2} (\bar{d}_i \sigma_{\mu\nu} d_j) (\bar{\ell} \sigma^{\mu\nu} \gamma_5 \ell').
\end{aligned} \tag{34}$$

In the above, e is the electric charge and $\sigma_{\mu\nu} = i[\gamma_\mu, \gamma_\nu]/2$. The set of primed operators ($X' = 7', 9', 10', S', P'$) comprises those of opposite chirality, and can be obtained by replacing $P_L \leftrightarrow P_R$ in the quark currents. The contribution of the right-handed current operators is negligible in the SM. Flavour universality of lepton-gauge interactions in the SM implies that the Wilson coefficients of operators $\mathcal{O}_i^{\ell\ell'}$ are universal for all lepton flavours ($\ell = e, \mu, \tau$), and the strict conservation of individual lepton flavour further precludes cLFV Wilson coefficients $C_i^{\ell\ell'}$ ($\ell \neq \ell'$).

In the present scalar leptoquark model, once the heavy degrees of freedom have been integrated out (under the assumption that $M_{t,W,Z}^2 \ll m_{h_1}^2$), the NP effective Hamiltonian is given by [91]

$$\mathcal{H}^{\text{NP}}(b \rightarrow s \ell^- \ell'^+) = -\frac{y_{b\ell'} y_{s\ell}^*}{m_{h_1}^2} (\bar{s} \gamma^\mu P_L b) (\bar{\ell} \gamma_\mu P_L \ell') + \text{H.c.}; \tag{35}$$

comparing the above with the operator basis of Eq. (33), it is possible to infer the following contributions to the Wilson coefficients

$$C_9^{\ell\ell'} = -C_{10}^{\ell\ell'} = \frac{\pi v^2}{\alpha_e V_{tb} V_{ts}^*} \frac{y_{b\ell'} y_{s\ell}^*}{m_{h_1}^2}. \tag{36}$$

The deviations from the SM lepton flavour universality imply that the modifications to the Wilson coefficients are necessarily non-universal for the muon and electron entries; the model-independent fit of [91] suggests the following corrections at the 1σ range:

$$\text{Re}[C_{9,\text{NP}}^{\mu\mu} - C_{10,\text{NP}}^{\mu\mu} - (\mu \leftrightarrow e)] \sim -1.1 \pm 0.3, \quad (37)$$

$$\text{Re}[C_{9'}^{\mu\mu} - C_{10'}^{\mu\mu} - (\mu \leftrightarrow e)] \sim 0.1 \pm 0.4, \quad (38)$$

(notice that the second constraint is compatible with zero, and can be fulfilled by setting $C_{9',10'}^{\mu\mu,ee} = 0$). In the present NP construction, leptoquark couplings to both muons and electrons are present, and are of left-handed nature. Given that $C_9^{\ell\ell'} = -C_{10}^{\ell\ell'}$ (cf. Eq. (36)), the best fit to the $C_{9,10}^{\mu\mu,ee}$ NP Wilson coefficients of Eq. (36) can be recast as

$$-1.4 \lesssim 2 \text{Re}[C_{9,\text{NP}}^{\mu\mu} - C_{9,\text{NP}}^{ee}] \lesssim -0.8. \quad (39)$$

Global fits to a large number of observables probing lepton flavour universality in relation to $b \rightarrow s\mu^\pm\mu^\mp$, $b \rightarrow se^\pm e^\mp$ and $b \rightarrow s\gamma$ processes also suggest NP scenarios consistent with the above fit to the LFUV $R_{K^{(*)}}$ observables. A common conclusion that can be generically drawn is that the NP responsible for the observed discrepancies in $b \rightarrow s$ data appears to predominantly couple to muons, and is strongly manifest in vector operators (as $\mathcal{O}_{9,10}^{\mu\mu}$). Recent studies and fits by a number of authors (see, e.g. [5, 92–95]) advocate NP contribution to $C_9^{\mu\mu}$ (~ -1) only, or then $SU(2)_L$ invariant scenarios ($C_9^{\mu\mu} = -C_{10}^{\mu\mu} \sim -0.6$) as preferred NP solutions to alleviate the tensions with the SM.

In terms of the h_1 leptoquark mass and couplings, the expression of Eq. (39) translates into the following condition [91]

$$0.64 \times 10^{-3} \lesssim \frac{\text{Re}[y_{b\mu} y_{s\mu}^* - y_{be} y_{se}^*]}{(m_{h_1}/1\text{TeV})^2} \lesssim 1.12 \times 10^{-3}. \quad (40)$$

In Fig. 3, for an illustrative value of $m_{h_1} = 1.5$ TeV, we display the $(y_{bl} y_{s\ell})$ parameter space consistent with the observed values of R_K and R_{K^*} at the 1σ level, in agreement with Eq. (40). The inset plot shows the regimes of $y_{b\mu}$ and $y_{s\mu}$ compatible with $R_{K^{(*)}}$ (also for $m_{h_1} = 1.5$ TeV, and for fixed values of the couplings to the electron, $y_{be} y_{se} = 2 \times 10^{-5}$).

5.2 Anomalies in $b \rightarrow c\ell^-\bar{\nu}_i$: $R_{D^{(*)}}$

Several experimental collaborations have also reported deviations from lepton flavour universality in association with $B \rightarrow D^*\ell\bar{\nu}$ decays (charged current $b \rightarrow c\ell\bar{\nu}_i$ transitions). A scalar charged leptoquark with non-trivial couplings to quarks and leptons can mediate $d_k \rightarrow u_j\ell\bar{\nu}_i$ transitions at the tree level, via the exchange of a charged $h_1^{1/3}$. The SM effective Hamiltonian governing these transitions is thus modified as follows:

$$\begin{aligned} \mathcal{H}_{\text{eff}}(d_k \rightarrow u_j\ell\bar{\nu}_i) &= \mathcal{H}_{\text{eff}}^{\text{SM}} + \mathcal{H}_{\text{eff}}^{\text{NP}} \\ &= \left[\frac{4G_F}{\sqrt{2}} V_{jk} U_{\ell i} - \frac{(yU)_{ki} (Vy^*)_{j\ell}}{2m_{h_1}^2} \right] (\bar{u}_j \gamma^\mu P_L d_k) (\bar{\ell} \gamma_\mu P_L \nu_i) + \text{H.c.} \\ &= \frac{4G_F}{\sqrt{2}} V_{jk} \left[U_{\ell i} - \frac{v^2}{4V_{cb} m_{h_1}^2} (yU)_{ki} (Vy^*)_{j\ell} \right] (\bar{u}_j \gamma^\mu P_L d_k) (\bar{\ell} \gamma_\mu P_L \nu_i) + \text{H.c.} \end{aligned} \quad (41)$$

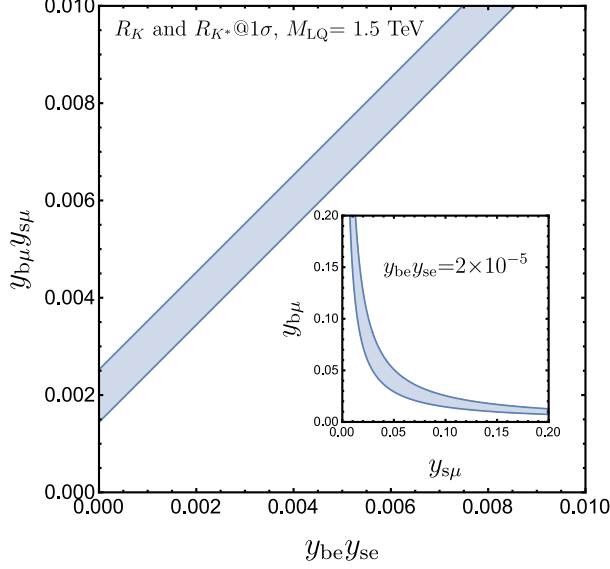


Figure 3: On the main plot, 1σ region in the $(y_{be} y_{se} - y_{b\mu} y_{s\mu})$ parameter space consistent with R_K and R_{K^*} data, cf. Eq. (40), for an example with $m_{h_1} = 1.5$ TeV. On the inset plot we display the $R_{K^{(*)}}$ allowed region in the $(y_{b\mu} - y_{s\mu})$ plane, for fixed values of the leptoquark electron Yukawa couplings $y_{be} y_{se} = 2 \times 10^{-5}$ (again for $m_{h_1} = 1.5$ TeV).

The experimentally measured decay probability is an incoherent sum over the (untagged) neutrino flavour i ; one thus finds

$$\begin{aligned}
 |\mathcal{A}(d_k \rightarrow u_j \ell \bar{\nu})|^2 &= \sum_i |\mathcal{A}_{\text{SM}}|^2 \left| U_{li} - \frac{v^2}{4 V_{jk} m_{h_1}^2} (yU)_{ki} (V y^*)_{j\ell} \right|^2 \\
 &= |\mathcal{A}_{\text{SM}}|^2 \left[1 + |x_{j\ell}|^2 \sum_i |y_{ki}|^2 - 2 \text{Re}(x_{j\ell} y_{k\ell}) \right], \quad (42)
 \end{aligned}$$

where $x_{j\ell} = (V y^*)_{j\ell} (v^2/4V_{cb}m_{h_1}^2)$, and in which one has used the unitarity of the PMNS matrix. The SM width for the decay $B \rightarrow D^* \ell \bar{\nu}$ (i.e., for $d_k = b$, $u_j = c$) will thus be corrected by an overall factor

$$\Gamma(B \rightarrow D^* \ell \bar{\nu}) = \Gamma_{\text{SM}}(B \rightarrow D^* \ell \bar{\nu}) \left[1 + |x_{c\ell}|^2 \sum_{i=e,\mu,\tau} |y_{bi}|^2 - 2 \text{Re}(x_{c\ell} y_{b\ell}) \right]. \quad (43)$$

Pure leptoquark contributions are suppressed by an additional $v^2/m_{h_1}^2$ factor with respect to the SM-NP interference term, and can be hence neglected as a first approximation.

Defining $R_{D^{(*)}}$ as the ratio of the decay widths of tau and muon modes - that is, $R_{D^{(*)}} = \text{BR}(B \rightarrow D^{(*)} \tau \bar{\nu})/\text{BR}(B \rightarrow D^{(*)} \mu \bar{\nu})$, one can further construct the double ratio

$$\frac{R_D}{R_{D,\text{SM}}} = \frac{R_{D^*}}{R_{D^*,\text{SM}}} = \frac{1 - 2 \text{Re}(x_{c\tau} y_{b\tau})}{1 - 2 \text{Re}(x_{c\mu} y_{b\mu})}, \quad (44)$$

(equal to one in the absence of NP). After combining current experimental world averages with

the SM predictions, the current anomalous data can be parametrised as

$$\frac{R_D}{R_{D,SM}} = 1.36 \pm 0.15, \quad \frac{R_{D^*}}{R_{D^*,SM}} = 1.21 \pm 0.06, \quad (45)$$

in which the statistical and systematical errors have been added in quadrature. Similar ratios comparing distinct final state lepton flavours can be built to test possible LFUV in the corresponding sectors. For example, the Belle Collaboration has reported measurements of the ratios $R_{D^{(*)}}^{\mu/e} = \text{BR}(B \rightarrow D^{(*)}\mu\bar{\nu})/\text{BR}(B \rightarrow D^{(*)}e\bar{\nu})$, which probe lepton flavour universality between electron and muon modes. The experimental values $R_D^{\mu/e,\text{exp}} = 0.995 \pm 0.022 \pm 0.039$ [96] and $R_{D^*}^{e/\mu,\text{exp}} = 1.04 \pm 0.05 \pm 0.01$ [97] are consistent with the SM expectation, ~ 1 . The averaged value of both measurements is $R_{D^{(*)}}^{\mu/e,\text{exp}} = 0.977 \pm 0.043$.

In the present leptoquark model, the ratio $R_{D^{(*)}}^{\mu/e}$ is given by the appropriately modified version of Eq. (44),

$$\frac{R_{D^{(*)}}^{\mu/e}}{R_{D^{(*)},SM}^{\mu/e}} = \frac{1 - 2 \text{Re}(x_{c\mu} y_{b\mu})}{1 - 2 \text{Re}(x_{ce} y_{be})}. \quad (46)$$

After having detailed the leptoquark contributions to the meson observables currently exhibiting a significant deviation from the SM expectation, we now address other processes which - being in agreement with SM predictions (negative searches or compatible measurements) can constrain the masses of the new states and their couplings.

6 Constraints from rare meson decays and oscillations

Various observables involving mesons lead to important bounds on leptoquark couplings; here we discuss the (leptoquark) NP contributions to leptonic and semi-leptonic meson decays (occurring at the tree level), and to meson oscillations and rare radiative decays, both at the loop level. The SM predictions and current experimental bounds for the processes here discussed are summarised in Table 2. The stringent bounds on NP contributions arising from the now observed decay $B_s \rightarrow \mu^+\mu^-$ are not discussed here, as they have been implicitly taken into account in defining the allowed ranges for $C_{10,\text{NP}}^{\mu\mu}$ and the $y_{22,23}$ Yukawa couplings in the previous section. Likewise, we do not include the constraints arising from semileptonic K -decays into charged dileptons ($K \rightarrow \pi\ell\ell$), as theoretical (SM) predictions are plagued by important uncertainties, and are not yet up to par with the precision of the experimental results (see for example [105, 106]).

6.1 Rare K and B meson decays: $K \rightarrow \pi\nu_\ell\bar{\nu}_{\ell'}$ and $B \rightarrow K^{(*)}\nu_\ell\bar{\nu}_{\ell'}$

The $s \rightarrow d\nu\nu$ and $b \rightarrow s\nu\nu$ transitions provide some of the most important constraints on NP scenarios aiming at addressing the anomalies in $R_{K^{(*)}}$ and $R_{D^{(*)}}$ data.

Following the convention of [107], at the quark level the $|\Delta S| = 1$ rare decays $K^+ (K_L) \rightarrow \pi^+ (\pi^0)\nu_\ell\bar{\nu}_{\ell'}$ and $B \rightarrow K^{(*)}\nu_\ell\bar{\nu}_{\ell'}$ can be described by the following short-distance effective Hamiltonian for $d_j \rightarrow d_i\nu_\ell\bar{\nu}_{\ell'}$ transitions [108, 109]

$$\begin{aligned} \mathcal{H}_{\text{eff}}(d_j \rightarrow d_i\nu_\ell\bar{\nu}_{\ell'}) = & -\frac{4G_F}{\sqrt{2}} V_{ti}^* V_{tj} \frac{\alpha_e}{2\pi} \left[C_{L,ij}^{\ell\ell'} (\bar{d}_i \gamma_\mu P_L d_j) (\bar{\nu}_\ell \gamma^\mu P_L \nu_{\ell'}) + \right. \\ & \left. + C_{R,ij}^{\ell\ell'} (\bar{d}_i \gamma_\mu P_R d_j) (\bar{\nu}_\ell \gamma^\mu P_L \nu_{\ell'}) \right] + \text{H.c.}, \quad (47) \end{aligned}$$

Observables	SM prediction	Experimental data
$\text{BR}(K^+ \rightarrow \pi^+ \nu \bar{\nu})$	$(8.4 \pm 1.0) \times 10^{-11}$ [98]	$17.3_{-10.5}^{+11.5} \times 10^{-11}$ [99] $< 11 \times 10^{-10}$ [100]
$\text{BR}(K_L \rightarrow \pi^0 \nu \bar{\nu})$	$(3.4 \pm 0.6) \times 10^{-11}$ [98]	$\leq 2.6 \times 10^{-8}$ [101]
$R_K^{\nu\nu}, R_{K^*}^{\nu\nu}$ $(B \rightarrow K^{(*)} \nu \bar{\nu})$	$R_{K^{(*)}}^{\nu\nu} = 1$	$R_K^{\nu\nu} < 3.9$ [102] $R_{K^*}^{\nu\nu} < 2.7$ [102]
$B_s^0 - \bar{B}_s^0$ (mixing parameters)	$\Delta_s = \Delta_s e^{i\phi_s} = 1$ $\phi_s = 0$	$ \Delta_s = 1.01_{-0.10}^{+0.17}$ [103], $\phi_s [^\circ] = 1.3_{-2.3}^{+2.3}$ [103]
$K^0 - \bar{K}^0$ $\Delta m_K / (10^{-15} \text{GeV})$	$3.1(1.2)$ [104]	$3.484(6)$ [1]
$\text{BR}(K_L \rightarrow \mu e)$	—	$< 4.7 \times 10^{-12}$ [1]
$\text{BR}(B_s \rightarrow \mu e)$	—	$< 1.1 \times 10^{-8}$ [1]

Table 2: Relevant observables and current experimental bounds for leptonic and semi-leptonic meson decays and neutral meson anti-meson oscillations discussed in this section.

in which i, j denote the down-type flavour content of the final and initial state meson, respectively. In the SM, only the lepton flavour conserving left-handed operator is present; the associated Wilson coefficient $C_{L,ij}^{\ell\ell}$ corresponding to a $d_j \rightarrow d_i$ transition is given by

$$C_{L,ij}^{\ell\ell, \text{SM}} = -\frac{1}{\sin^2 \theta_w} \left(X_t^{\text{SM}} + \frac{V_{ci}^* V_{cj}}{V_{ti}^* V_{tj}} X_c^\ell \right). \quad (48)$$

In the above, X_t^{SM} and X_c^ℓ ($\ell = e, \mu, \tau$) are the loop functions associated with the (lepton flavour conserving) contributions from the top and charm quarks, respectively. In the SM, computations of the top loop function (including Next-to-Leading Order QCD corrections [110–112] and the full two-loop electroweak corrections [113]) have led to the result $X_t^{\text{SM}} = 1.481(9)$ [98]; the charm loop functions X_c^ℓ have been computed at NLO [112, 114] and at Next-to-NLO [115, 116], and their numerical value is given by $\frac{1}{3} \sum_\ell X_c^\ell / |V_{us}|^4 = 0.365 \pm 0.012$.

Once the heavy leptoquark degrees of freedom have been integrated out, the general effective Hamiltonian describing the NP contribution to $d_j \rightarrow d_i \nu_\ell \bar{\nu}_{\ell'}$ processes induced by h_1 is given by

$$\mathcal{H}_{\text{eff}}^{\text{LQ}}(d_j \rightarrow d_i \nu_\ell \bar{\nu}_{\ell'}) = -\frac{(yU)_{j\ell'} (yU)_{i\ell}^*}{2m_{h_1}^2} (\bar{d}_i \gamma_\mu P_L d_j) (\bar{\nu}_\ell \gamma^\mu P_L \nu_{\ell'}), \quad (49)$$

and comparison with Eq. (47) leads to the following NP Wilson coefficient,

$$C_{L,ij}^{\ell\ell', \text{LQ}} = \frac{\pi v^2}{\alpha_e V_{ti}^* V_{tj}} \frac{(yU)_{i\ell}^* (yU)_{j\ell'}}{2m_{h_1}^2}, \quad (50)$$

in which we notice the presence of the PMNS matrix U , and the possibility that the tree level NP contribution, via the exchange of $h_1^{1/3}$, may lead to different lepton flavours in the final state, i.e. $\ell \neq \ell'$.

$K \rightarrow \pi \nu_\ell \bar{\nu}_{\ell'}$ decays

The branching fraction for $K^+ \rightarrow \pi^+ \nu_\ell \bar{\nu}_{\ell'}$ (corresponding to setting $i = d, j = s$ in the previous discussion) is given by [108, 109]

$$\text{BR}(K^+ \rightarrow \pi^+ \nu_\ell \bar{\nu}_{\ell'}) = \frac{\kappa_+ (1 + \Delta_{\text{em}})}{3} \sum_{\ell, \ell' = e, \mu, \tau} \left| \frac{V_{ts}^* V_{td}}{|V_{us}|^5} X_t^{\ell\ell'} + \frac{V_{cs}^* V_{cd}}{|V_{us}|} \delta_{\ell\ell'} \left(\frac{X_c^\ell}{|V_{us}|^4} + \Delta_{P_{c,u}^\ell} \right) \right|^2, \quad (51)$$

in which $\kappa_+ = 5.173(25) \times 10^{-11} (|V_{us}|/0.225)^8$, $\Delta_{\text{em}} = -0.003$ is the electromagnetic correction from photon exchanges and $\Delta_{P_{c,u}^\ell} = 0.04(2)$ denotes the long-distance contribution from light quark loops, computed in [117]. The loop function associated with NP exchanges, $X_t^{\ell\ell'}$, is given by

$$X_t^{\ell\ell'} = X_t^{\text{SM}} \delta_{\ell\ell'} - \sin^2 \theta_w C_{L, sd}^{\ell\ell', \text{LQ}}. \quad (52)$$

Notice from both Eqs. (51, 52) that the SM top and charm contributions are lepton flavour conserving. Experimentally, the measurement of the charged kaon decay mode [99],

$$\text{BR}(K^+ \rightarrow \pi^+ \nu \bar{\nu})_{\text{exp}} = 17.3_{-10.5}^{+11.5} \times 10^{-11}, \quad (53)$$

is expected to be improved in the near future by the results of the NA62 collaboration. The NA62 recent measurement [100] (one event) $\text{BR}(K^+ \rightarrow \pi^+ \nu \bar{\nu})_{\text{exp}} = 28_{-23}^{+44} \times 10^{-11}$ still suffers from large statistical uncertainties, but these are expected to improve by an order of magnitude in coming months. The experimental bounds will allow to better constrain $X_t^{\ell\ell'}$, and hence the leptoquark contributions, encoded in $C_{L, ij}^{\ell\ell', \text{LQ}}$.

$K_L \rightarrow \pi^0 \nu_\ell \nu_{\ell'}$ decays

The branching fraction for the neutral mode $K_L \rightarrow \pi^0 \nu_\ell \nu_{\ell'}$ can be written as [108, 109]

$$\text{BR}(K_L \rightarrow \pi^0 \nu_\ell \nu_{\ell'}) = \frac{\kappa_L}{3} \sum_{\ell, \ell' = e, \mu, \tau} \left[\text{Im} \left(\frac{V_{ts}^* V_{td}}{|V_{us}|^5} X_t^{\ell\ell'} \right) \right]^2, \quad (54)$$

with $\kappa_L = 2.231(13) \times 10^{-10} (|V_{us}|/0.225)^8$ in the framework of the SM. Concerning the experimental status, only a 90% C.L. bound has been reported for the decay [101]

$$\text{BR}(K_L \rightarrow \pi^0 \nu \bar{\nu})_{\text{exp}} \leq 2.6 \times 10^{-8}, \quad (55)$$

which - as occurring for the charged decay modes - can also be used to constrain $X_t^{\ell\ell'}$ and $C_{L, ij}^{\ell\ell', \text{LQ}}$ (albeit leading to weaker constraints than those inferred from the $K^+ \rightarrow \pi^+ \nu \bar{\nu}$ mode).

$B \rightarrow K^{(*)} \nu_\ell \bar{\nu}_{\ell'}$

The branching ratio for the rare B decay can be obtained by considering the general expressions for the effective Hamiltonian and NP Wilson coefficients, respectively given in Eqs. (47, 50), with $i = s, j = b$. It proves convenient to consider the following ratios $R_{K^{(*)}}^{\nu\nu} = \Gamma_{\text{SM} + \text{NP}}(B \rightarrow K^{(*)} \nu \nu) / \Gamma_{\text{SM}}(B \rightarrow K^{(*)} \nu \nu)$, which are then given by

$$R_K^{\nu\nu} = R_{K^*}^{\nu\nu} = \frac{1}{3 |C_{L, bs}|^2} \sum_{\ell, \ell'} \left| C_{L, bs}^{\ell\ell, \text{SM}} \delta_{\ell\ell'} + C_{L, bs}^{\ell\ell', \text{LQ}} \right|^2, \quad (56)$$

in which $C_{L,SM}^{\ell\ell} = -6.38(6)$ (for each neutrino flavour) [113]. The above expression can be explicitly cast in terms of the leptoquark masses and couplings as follows:

$$R_{K^{(*)}}^{\nu\nu} = \frac{1}{3 |C_{L,bs}^{\ell\ell,SM}|^2} \left[3 |C_{L,bs}^{\ell\ell,SM}|^2 + \sum_{\ell \neq \ell'} \left| \left(\frac{\pi v^2}{\alpha_e V_{tb} V_{ts}^*} \right) \frac{y_{b\ell'} y_{s\ell}^*}{2 m_{h_1}^2} \right|^2 + \sum_{\ell=\ell'} \left\{ \left| \left(\frac{\pi v^2}{\alpha_e V_{tb} V_{ts}^*} \right) \frac{y_{b\ell} y_{s\ell}^*}{2 m_{h_1}^2} \right|^2 + 2 \operatorname{Re} \left[C_{L,bs}^{\ell\ell,SM*} \left(\frac{\pi v^2}{\alpha_e V_{tb} V_{ts}^*} \right) \frac{y_{b\ell} y_{s\ell}^*}{2 m_{h_1}^2} \right] \right\} \right]. \quad (57)$$

The SM predictions for each of the modes are $\operatorname{BR}(B^+ \rightarrow K^+ \nu \bar{\nu}) = (4.0 \pm 0.5) \times 10^{-6}$ [107] and $\operatorname{BR}(B^0 \rightarrow K^{*0} \nu \bar{\nu}) = (9.2 \pm 1.0) \times 10^{-6}$ [107].

The latest experimental data from Belle [102] allows to infer the following bound, $R_{K^{(*)}}^{\nu\nu} < 3.9(2.7)$ at 90% C.L., which can be used to constrain combinations of leptoquark couplings (lepton flavour conserving and violating) as given in Eq. (57).

6.2 Neutral meson mixings and oscillations

Contributions to neutral meson mixings, $P - \bar{P}$ with $P = B_s^0, B_d^0, K^0$, arise both from SM box diagrams involving top and W 's, and from NP box diagrams involving charged (neutral) leptons and $h_1^{4/3}(h_1^{1/3})$ leptoquarks. These contributions can be described in terms of the following effective Hamiltonian for $|\Delta F| = 2$ transitions

$$\mathcal{H}_P = (C_P^{\text{SM}} + C_P^{\text{NP}}) (\bar{d}_i \gamma^\mu P_L d_j) (\bar{d}_i \gamma_\mu P_L d_j) + \text{H.c.}, \quad (58)$$

where [57]

$$C_P^{\text{NP}} = \frac{3}{128 \pi^2 m_{h_1}^2} \left(\sum_{\ell} y_{i\ell}^* y_{j\ell} \right)^2, \quad (59)$$

with $\{i, j\}$ respectively denoting $\{b, s\}$, $\{b, d\}$ or $\{d, s\}$ for $P = B_s^0, B_d^0$ or K^0 mesons.

Let us begin by discussing B_s^0 mixing, which is potentially the process most sensitive to the couplings $y_{b\ell}$ and $y_{s\ell}$ which are at the origin of the $R_{K^{(*)}}$ anomalies. Following [103, 118, 119], one can define the ratio of the total contribution (NP and SM) to the SM one

$$\Delta_s = |\Delta_s| e^{i\phi_s} = \frac{\langle B_s | \mathcal{H}_{B_s} | \bar{B}_s \rangle}{\langle B_s | \mathcal{H}_{B_s}^{\text{SM}} | \bar{B}_s \rangle} = 1 + \frac{C_{B_s}^{\text{NP}}}{C_{B_s}^{\text{SM}}} \equiv 1 + p_s. \quad (60)$$

In the leptoquark model we consider, the relative NP contribution p_s can be cast as

$$p_s = \frac{3 (\sum_{\ell} y_{b\ell} y_{s\ell}^*)^2}{32 m_{h_1}^2 G_F^2 M_W^2 S_0(x_t) (V_{tb} V_{ts}^*)^2}, \quad (61)$$

where $S_0(x_t) = 2.35$ is the Inami-Lim function for the SM top quark box, with $x_t = M_t^2/M_W^2$ [120, 121]. Current global fits are compatible with the SM value ($\Delta_s^{\text{SM}} = 1$): CKMfitter reports $|\Delta_s| = 1.01_{-0.10}^{+0.17}$, $\phi_s[^\circ] = 1.3_{-2.3}^{+2.3}$ [103], while for UTfit one has $|\Delta_s| = 1.070 \pm 0.088$, $\phi_s[^\circ] = 0.054 \pm 0.951$ [119]. Both analyses obtain their tightest 1σ constraints for imaginary NP contributions (i.e., $\arg p_s = -\pi/2$): $|p_s| < 0.016$. In our study, and for simplicity, we will assume real Yukawa couplings $y_{q\ell}$ and a real p_s . In this case one has $p_s \geq 0$, and both analyses lead to

$p_s < p_s^{\max} \approx 0.17$, which translates into the following 1σ upper bound for the (real) h_1 leptoquark couplings:

$$\left| \sum_{\ell} y_{b\ell} y_{s\ell} \right| \lesssim 0.079 \frac{m_{h_1}}{\text{TeV}} \sqrt{\frac{p_s^{\max}}{0.17}}. \quad (62)$$

Following the same global analyses, a similar bound can be inferred from data on B_d^0 mixing (still in the case of real couplings), which leads to $p_d < p_d^{\max} \approx 0.13$. One thus has

$$\left| \sum_{\ell} y_{b\ell} y_{d\ell} \right| \lesssim 0.069 \frac{m_{h_1}}{\text{TeV}} \sqrt{\frac{p_d^{\max}}{0.13}}. \quad (63)$$

For the case of $K^0 - \bar{K}^0$ mixing, the SM effective coupling can be expressed as

$$C_K^{\text{SM}} = \frac{G_F^2 M_W^2}{4\pi^2} F^*(x_c, x_t) \quad (64)$$

where $F(x_c, x_t)$ denotes the contribution of the distinct Inami-Lim functions, and is defined as

$$F(x_c, x_t) = (V_{cs}^* V_{cd})^2 \eta_{cc} S_0(x_c) + (V_{ts}^* V_{td})^2 \eta_{tt} S_0(x_t) + 2 V_{ts}^* V_{td} V_{cs}^* V_{cd} \eta_{ct} S_0(x_c, x_t), \quad (65)$$

with $S_0(x_c) \approx x_c + O(x_c^2) = m_c^2/M_W^2$ [120, 121]; the coefficients $\eta_{cc} = 1.87(76)$, $\eta_{tt} = 0.5765(65)$ and $\eta_{ct} = 0.496(47)$ encode NNLO QCD corrections [104, 122–124]. The last two terms in Eq. (65) can be safely neglected (as they are CKM-suppressed); the first (and dominant) term is associated to important theoretical uncertainties, $\mathcal{O}(40\%)$. From Eq. (59), the leptoquark contribution can be written as

$$p_K = \frac{C_K^{\text{NP}}}{C_K^{\text{SM}}} = \frac{3 \eta_{tt} \tilde{r} (\sum_{\ell} y_{s\ell} y_{d\ell}^*)^2}{32 m_{h_1}^2 G_F^2 M_W^2 S_0(x_c) \eta_{cc} (V_{cs} V_{cd}^*)^2}, \quad (66)$$

in which $\tilde{r} \approx 0.95$ allows to take into account the difference between the relevant scales (M_t and m_{h_1}) [125].

Real couplings $y_{q\ell}$ only affect $\Delta m_K = \text{Re}\langle \bar{K}^0 | \mathcal{H}_K | K^0 \rangle / m_K$. Taking into account only the (dominant) first term of Eq. (65), the SM short distance contribution (cf. Eq. (64)) gives [104, 126]

$$(\Delta m_K)_{\text{SM}} = (3.1 \pm 1.2) \times 10^{-15} \text{GeV} = (0.89 \pm 0.34) (\Delta m_K)_{\text{exp}} \quad (67)$$

Comparing $(\Delta m_K)_{\text{exp}}$ with the theoretical prediction $((\Delta m_K)_{\text{SM}} + (\Delta m_K)_{\text{NP}} + (\Delta m_K)_{\text{LD}})$, thus allows to obtain a conservative upper bound, $p_K < p_K^{\max} \approx 0.45/0.55 = 0.81$. Leading to the latter limit, one has taken the lowest values of both $(\Delta m_K)_{\text{SM}}$ ($\sim 55\%$) and the long distance (LD) contributions $(\Delta m_K)_{\text{LD}}$, which are hard to evaluate but are expected to be positive like p_k [126]. This translates into an upper bound on the leptoquark couplings:

$$\left| \sum_{\ell} y_{s\ell} y_{d\ell} \right| \lesssim 0.014 \frac{m_{h_1}}{\text{TeV}} \sqrt{\frac{p_K^{\max}}{0.81}}. \quad (68)$$

6.3 Leptonic decays of pseudoscalar mesons $P \rightarrow \ell^- \ell'^+$

The leptonic decays of pseudoscalar mesons are known to provide stringent constraints on models of NP with modified lepton (and/or quark) sectors; leptoquark models are no exception, and in what follows we discuss some relevant modes of K and B mesons.

Leptonic B_s meson decays $B_{(s)}^0 \rightarrow \ell^\pm \ell^\mp$ are well predicted in the SM (the only hadronic uncertainty coming from the decay constant f_{B_s}). At present, only the $B_s \rightarrow \mu^+ \mu^-$ decay mode has been observed, and it is in agreement with the SM. The LHC collaborations have reported values for its branching fraction of $(2.8_{-0.6}^{+0.7}) \times 10^{-6}$ [127, 128]. As mentioned before, these bounds have been taken into account upon saturation of the B decay anomalies.

For both K and B mesons, the cLFV leptonic decays have been shown to lead to important constraints on NP models: the cLFV B decay modes are particularly relevant for leptoquark SM extensions [129]; although the hard to quantify long-distance QCD corrections render non-trivial an estimation of the leptonic K_L decays [130]), the upper bounds on the cLFV mode $K_L \rightarrow \mu^\pm e^\mp$ prove to be one of the most stringent constraints on the couplings of leptoquarks to the first two generations of leptons and down-type quarks.

Following the effective Hamiltonian conventions adopted in Eq. (33), the decay width of $P \rightarrow \ell^\pm \ell'^\mp$ is governed by the $\mathcal{O}_9^{ij;\ell\ell'}$ and $\mathcal{O}_{10}^{ij;\ell\ell'}$ operators. In terms of the corresponding Wilson coefficients $C_{9,10}^{ij;\ell\ell'}$, the decay width can be written [129]

$$\begin{aligned} \Gamma_{P \rightarrow \ell - \ell'^+} &= f_P^2 m_P^3 \frac{G_F^2 \alpha_e^2}{64 \pi^3} |V_{qj} V_{qi}^*|^2 \beta(m_P, m_\ell, m_{\ell'}) \times \\ &\times \left[\left(1 - \frac{(m_\ell + m_{\ell'})^2}{m_P^2} \right) \left| \frac{m_P}{(m_i + m_j)} (C_S^{ij;\ell\ell'} - C_{S'}^{ij;\ell\ell'}) + \frac{(m_\ell - m_{\ell'})}{m_P} (C_9^{ij;\ell\ell'} - C_{9'}^{ij;\ell\ell'}) \right|^2 + \right. \\ &\left. + \left(1 - \frac{(m_\ell - m_{\ell'})^2}{m_P^2} \right) \left| \frac{m_P}{(m_i + m_j)} (C_P^{ij;\ell\ell'} - C_{P'}^{ij;\ell\ell'}) + \frac{(m_\ell + m_{\ell'})}{m_P} (C_{10}^{ij;\ell\ell'} - C_{10'}^{ij;\ell\ell'}) \right|^2 \right], \end{aligned} \quad (69)$$

in which $m_{i,j}$ denotes the mass of the meson valence quarks, the index q refers to up-type quarks (the sum being dominated by the top quark contribution), and one defines

$$\beta(m_P, m_\ell, m_{\ell'}) = \sqrt{[1 - (m_\ell - m_{\ell'})^2/m_P^2][1 - (m_\ell + m_{\ell'})^2/m_P^2]}. \quad (70)$$

7 Charged lepton flavour violating processes

Due to the presence of new states with non-negligible couplings to neutral and charged leptons, which are a source of LFUV, one expects that the model under consideration will give rise to important contributions to cLFV observables.

While most cLFV decays correspond to higher order (loop) processes, it is important to notice that transitions occurring in the presence of matter, such as neutrinoless muon-electron conversion in nuclei can now occur at the tree level. In the following, we address the contributions of the model to several cLFV observables⁶, whose experimental status (current bounds and future sensitivities) is summarised in Table 3. The bounds on leptonic observables will give rise to stringent constraints on the parameter space of the model: other than neutrino oscillation data, bounds on several lepton flavour violating observables will play a significant rôle in identifying the regimes which can successfully lead to an explanation of the B meson anomalies.

⁶In what concerns three-body decays we focus our discussion on the case of same-flavour final lepton state, i.e., $\ell \rightarrow 3\ell'$.

⁷For a relevant discussion concerning the future perspectives of the searches for $\mu \rightarrow e\gamma$ process see [133].

cLFV process	Current experimental bound	Future sensitivity
BR($\mu \rightarrow e\gamma$)	4.2×10^{-13} (MEG [131])	6×10^{-14} (MEG II [132]) ⁷
BR($\tau \rightarrow e\gamma$)	3.3×10^{-8} (BaBar [134])	10^{-9} (Super B [135])
BR($\tau \rightarrow \mu\gamma$)	4.4×10^{-8} (BaBar [134])	10^{-9} (Super B [135])
BR($\mu \rightarrow 3e$)	1.0×10^{-12} (SINDRUM [136])	$10^{-15(16)}$ (Mu3e [137])
BR($\tau \rightarrow 3e$)	2.7×10^{-8} (Belle [138])	10^{-9} (Super B [135])
BR($\tau \rightarrow 3\mu$)	3.3×10^{-8} (Belle [138])	10^{-9} (Super B [135])
CR($\mu - e, N$)	7×10^{-13} (Au, SINDRUM [139])	10^{-14} (SiC, DeeMe [140]) $10^{-15(-17)}$ (Al, COMET [141]) 3×10^{-17} (Al, Mu2e [142]) 10^{-18} (Ti, PRISM/PRIME [143])

Table 3: Current experimental bounds and future sensitivities of cLFV processes included in the analysis.

7.1 Radiative decays $\ell \rightarrow \ell' \gamma$

In the present model, radiative charged lepton decays are induced at the loop level (h_1 leptoquarks and quarks running in the loop). The effective Lagrangian for $\ell \rightarrow \ell' \gamma$ decays can be written as [144]

$$\mathcal{L}_{\text{eff}}^{\ell \rightarrow \ell' \gamma} = -\frac{4G_F}{\sqrt{2}} \bar{\ell}' \sigma^{\mu\nu} F_{\mu\nu} \left(C_L^{\ell\ell'} P_L + C_R^{\ell\ell'} P_R \right) \ell + \text{H.c.}, \quad (71)$$

with $F_{\mu\nu}$ the electromagnetic field strength. The flavour violating coefficients can be cast as

$$C_{L(R)}^{\ell\ell'} = \frac{e}{4\sqrt{2}G_F} \sigma_{L(R)}^{\ell\ell'}; \quad (72)$$

the new states and interactions give rise to the following effective coefficients $\sigma_{L(R)}^{\ell\ell'}$,

$$\begin{aligned} \sigma_L^{\ell\ell'} &= \frac{3}{16\pi^2 m_{h_1}^2} \sum_q X_{q\ell'}^* X_{q\ell} m_{\ell'} [Q_S f_S(x_q) - f_F(x_q)], \\ \sigma_R^{\ell\ell'} &= \frac{3}{16\pi^2 m_{h_1}^2} \sum_q X_{q\ell'}^* X_{q\ell} m_{\ell} [Q_S f_S(x_q) - f_F(x_q)]. \end{aligned} \quad (73)$$

In the above, $X_{q\ell} \equiv -\sqrt{2}y_{q\ell}$ and $Q_S = 4/3$ for down-type quarks ($q = d$), while $X_{q\ell} \equiv -V_{qq'}^* y_{q'\ell}$ and $Q_S = 1/3$ for up-type quarks ($q = u$). The loop functions, cast in terms of $x_q = m_q^2/m_{h_1}^2$, are given by

$$f_S(x) = \frac{x+1}{4(1-x)^2} + \frac{x \log x}{2(1-x)^3}, \quad f_F(x) = \frac{x^2 - 5x - 2}{12(x-1)^3} + \frac{x \log x}{2(x-1)^4}. \quad (74)$$

Finally, the cLFV radiative decay width is given by

$$\Gamma(\ell \rightarrow \ell' \gamma) = \frac{\alpha_e m_{\ell}^3 (1 - m_{\ell'}^2/m_{\ell}^2)^3}{4} \left(|\sigma_L^{\ell\ell'}|^2 + |\sigma_R^{\ell\ell'}|^2 \right). \quad (75)$$

7.2 Three body decays $\ell \rightarrow \ell' \ell' \ell'$

The photonic interactions at the source of the radiative decays (parametrised by the couplings $C_{L,R}^{\ell\ell'}$, see Eq. (71)) will also induce the three-body cLFV decays; moreover, direct four-fermion interactions are responsible for additional contributions.

Following [145, 146], the low-energy effective Lagrangian including the four-fermion (contact) operators responsible for $\ell \rightarrow \ell' \ell' \ell'$ decays can be written as

$$\begin{aligned} \mathcal{L}_{\ell \rightarrow \ell' \ell' \ell'} = & -\frac{4G_F}{\sqrt{2}} \left[g_1 (\bar{\ell}' P_L \ell) (\bar{\ell}' P_L \ell') + g_2 (\bar{\ell}' P_R \ell) (\bar{\ell}' P_R \ell') + \right. \\ & + g_3 (\bar{\ell}' \gamma^\mu P_R \ell) (\bar{\ell}' \gamma_\mu P_R \ell') + g_4 (\bar{\ell}' \gamma^\mu P_L \ell) (\bar{\ell}' \gamma_\mu P_L \ell') + \\ & \left. + g_5 (\bar{\ell}' \gamma^\mu P_R \ell) (\bar{\ell}' \gamma_\mu P_L \ell') + g_6 (\bar{\ell}' \gamma^\mu P_L \ell) (\bar{\ell}' \gamma_\mu P_R \ell') \right] + \text{H.c.} \end{aligned} \quad (76)$$

In the model under study, there are several types of diagrams contributing to the 3-body cLFV decays: photon penguins (dipole and off-shell ‘‘anapole’’), Z penguins and box diagrams, all due to flavour violating interactions involving the scalar leptoquark h_1 and quarks. Neglecting Higgs-mediated exchanges, the distinct diagrams will give rise to non-vanishing contributions to the dipole operators ($C_{L,R}^{\ell\ell'}$), as well as to g_3 , g_4 , g_5 and g_6 . The box and the Z penguin diagrams contribute to g_4 and g_6 as follows [57]

$$\begin{aligned} g_4^{\text{box},Z} &= \frac{\sqrt{2}}{4G_F} \frac{3(y^\dagger y)_{\ell\ell'}}{(4\pi)^2 m_{h_1}^2} \left[(y^\dagger y)_{\ell\ell'} + \frac{\sqrt{2}}{9} G_F M_W^2 (2 - 3 \cos^2 \theta_w - 3 \log x - 3\pi i) \right], \\ g_6^{\text{box},Z} &= \frac{\sqrt{2}}{4G_F} \frac{3(y^\dagger y)_{\ell\ell'}}{(4\pi)^2 m_{h_1}^2} \frac{2\sqrt{2}}{9} G_F M_Z^2 \sin^2 \theta_w (2 - 3 \cos^2 \theta_w - 3 \log x - 3\pi i), \end{aligned} \quad (77)$$

in which $x = M_Z^2/m_{h_1}^2$. The off-shell γ -penguin diagrams induce non-vanishing contributions to $g_{3,5}$ and $g_{4,6}$, which are given by [145]

$$\begin{aligned} g_3^\gamma &= g_5^\gamma = \frac{\sqrt{2}e^2}{4G_F m_\mu^2} \left[\tilde{f}_{E0}(0) + \tilde{f}_{M0}(0) \right], \\ g_4^\gamma &= g_6^\gamma = \frac{\sqrt{2}e^2}{4G_F m_\mu^2} \left[\tilde{f}_{E0}(0) - \tilde{f}_{M0}(0) \right], \end{aligned} \quad (78)$$

in which the form factors can be cast as

$$f_{E0}(q^2) = \frac{q^2}{m_\mu^2} \tilde{f}_{E0}(q^2), \quad f_{M0}(q^2) = \frac{q^2}{m_\mu^2} \tilde{f}_{M0}(q^2), \quad (79)$$

and are defined in such a way that $\tilde{f}_{E0}(q^2)$ and $\tilde{f}_{M0}(q^2)$ are finite at $q^2 \rightarrow 0$ (q being the four-momentum transfer). The cLFV loops involving h_1 leptoquarks and up (or down) quarks contribute to the off-shell penguin form factors as follows

$$\begin{aligned} f_{E0}^{i=u} &= -f_{M0}^{i=u} = -\frac{\sum_i X_{i\ell'}^* X_{i\ell}}{3(4\pi)^2} \frac{(-q^2)}{m_{h_1}^2} \left(\ln \frac{(-q^2)}{m_{h_1}^2} + f_\gamma(r_i) - \frac{1}{12} \right), \\ f_{E0}^{i=d} &= -f_{M0}^{i=d} = -\frac{\sum_i X_{i\ell'}^* X_{i\ell}}{6(4\pi)^2} \frac{(-q^2)}{m_{h_1}^2} \left(\ln \frac{(-q^2)}{m_{h_1}^2} + f_\gamma(r_i) - \frac{1}{3} \right). \end{aligned} \quad (80)$$

We recall that in the above $X_{i\ell} \equiv -\sqrt{2}y_{q\ell}$ for $i = d$, and $X_{i\ell} \equiv -V_{ij}^*y_{j\ell}$ for $i = u$; the loop function $f_\gamma(r_i)$ is given by

$$f_\gamma(r_i) = -\frac{1}{3} + 4r_i + \ln r_i + (1 - 2r_i) \sqrt{1 + 4r_i} \ln \left(\frac{\sqrt{1 + 4r_i} + 1}{\sqrt{1 + 4r_i} - 1} \right). \quad (81)$$

with $r_i = m_i^2/(-q^2)$, where i denotes the quark in the loop.

As an example, for the case of $\mu \rightarrow 3e$ decays, one is led to the following branching ratio [145,146]

$$\begin{aligned} \text{BR}(\mu \rightarrow eee) &= 2 (|g_3|^2 + |g_4|^2) + |g_5|^2 + |g_6|^2 + \\ &+ 8 e \text{Re} [C_R^{\mu e} (2g_4^* + g_6^*) + C_L^{\mu e} (2g_3^* + g_5^*)] + \\ &+ \frac{32 e^2}{m_\mu^2} \left\{ \ln \frac{m_\mu^2}{m_e^2} - \frac{11}{4} \right\} (|C_R^{\mu e}|^2 + |C_L^{\mu e}|^2). \end{aligned} \quad (82)$$

Analogous expressions can be easily inferred for the other cLFV 3-body decay channels.

7.3 Neutrinoless μ - e conversion in Nuclei

One of the most important constraints on SM extensions with scalar leptoquarks⁸ arises from the nuclear assisted $\mu - e$ conversion. Phenomenologically - and contrary to other cLFV transitions which remain loop-mediated processes - neutrinoless $\mu - e$ conversion can occur at the tree-level in the presence of lepton-quark-leptoquark interactions. Moreover, as summarised in Table 3, the experimental prospects for this cLFV observable are particularly promising: not only current bounds (obtained for Gold nuclei) are already $\mathcal{O}(10^{-13})$, but in the near future several dedicated experiments should bring the sensitivity down to $\mathcal{O}(10^{-17,-18})$ [142,143]. The conversion ratio is defined as

$$\text{CR}(\mu - e, \text{N}) \equiv \frac{\Gamma(\mu - e, \text{N})}{\Gamma_{\text{capture}}(Z)} \quad (83)$$

in which $\Gamma_{\text{capture}}(Z)$ denotes the capture rate for a nucleus with atomic number Z , and $\Gamma(\mu - e, \text{N})$ is the cLFV width, which can be generically cast as follows [144,148]:

$$\Gamma^{\mu-e} = 2G_F^2 \left| \frac{C_R^{\mu e*}}{m_\mu} D + \left(2g_{LV}^{(u)} + g_{LV}^{(d)} \right) V^{(p)} + \left(g_{LV}^{(u)} + 2g_{LV}^{(d)} \right) V^{(n)} \right|^2 + 2G_F^2 \left| \frac{C_L^{\mu e*}}{m_\mu} D \right|^2, \quad (84)$$

where the (tree-level) flavour violation is encoded in the following quantities [144]

$$g_{LV}^{(d)} = -4 \frac{v^2}{2m_{h_1}^2} y_{d\ell} y_{d\ell}^*, \quad g_{LV}^{(u)} = -4 \frac{v^2}{2m_{h_1}^2} (V^T y)_{u\ell} (V^T y)_{u\ell}^*. \quad (85)$$

Other than the (dominant) tree-level exchanges, we have also included the photon-penguin contributions in the expression of the conversion width⁹; these are associated with the $C_{L(R)}^{\ell\ell'}$ coefficients, which have been previously defined in Eq. (72). The relevant nuclear information (nuclear form factors and averages over the atomic electric field) are encoded in the D , $V^{(p)}$ and $V^{(n)}$ form factors. The latter overlap integrals have been numerically estimated for various nuclei [148]; Table 4

⁸Recently, neutrinoless $\mu - e$ conversion in nuclei, in particular the comparative study of spin-independent versus spin-dependent contributions, has been explored as a powerful means of disentangling distinct leptoquark realisations [147].

⁹These are typically responsible for contributions to the conversion rate which are a factor of 10^{-3} smaller than the tree-level contribution; box diagrams have also been found to provide negligible contributions.

Nucleus	$D[m_\mu^{5/2}]$	$V^{(p)}[m_\mu^{5/2}]$	$V^{(n)}[m_\mu^{5/2}]$	$\Gamma_{\text{capture}}[10^6 \text{s}^{-1}]$
$^{197}_{79}\text{Au}$	0.189	0.0974	0.146	13.07
$^{27}_{13}\text{Al}$	0.0362	0.0161	0.0173	0.7054

Table 4: Overlap integrals (normalised to units of $m_\mu^{5/2}$) and total capture rates for Gold and Aluminium [148].

summarises some of the above quantities for Gold and Aluminium nuclei (in units of $m_\mu^{5/2}$), as well as the corresponding capture widths.

Current bounds (from Gold nuclei) already allow to infer the following stringent constraints [144]: $g_{LV}^{(u)} < 8 \times 10^{-8}$ and $g_{LV}^{(d)} < 12 \times 10^{-8}$.

7.4 Further leptonic observables

Other tensions between SM predictions and observation have also fuelled the need for NP. One such case is the anomalous magnetic moment of the muon; we notice here that the present leptoquark construction does provide a non-vanishing contribution to $(g - 2)_\mu$, albeit with the “wrong” sign [57], so that it cannot ease the current discrepancy.

Being a priori complex, the leptoquark couplings can also induce contributions to the electric dipole moments of quarks and leptons, at the two loop level. Although these could possibly allow to further constrain the couplings (in particular, the CP violating phases), such a detailed analysis lies beyond the scope of the current work.

8 Accommodating B -anomalies, dark matter and neutrino data

In the previous sections we have discussed in detail the distinct observations and experimental tensions that the present leptoquark model is called upon to explain; moreover, we have also addressed a comprehensive set of observables (encompassing numerous quark and lepton flavour transitions) that are expected to lead to important constraints on specific realisations of the model.

In this section, we finally identify the different regimes thus allowing to:

- (i) accommodate the latest data on neutrino oscillation parameters;
- (ii) account for a correct relic abundance for the dark matter candidate;
- (iii) explain the $R_{K^{(*)}}$ and $R_{D^{(*)}}$ anomalies;
- (iv) be compatible with all available bounds on leptoquark couplings and masses arising from direct searches, as well as from the relevant leptonic and semi-leptonic meson decays and transitions (including neutral meson oscillations and rare meson decays) - both tree level and higher order processes -, and cLFV processes (radiative and three-body decays, and $\mu - e$ conversion in nuclei).

The results of the approximative numerical study of Section 4 suggested that a viable dark matter candidate could be obtained for a LZoP (the lightest $\Sigma^{1,0}$) mass in the range $2.425 \text{ TeV} \lesssim m_\Sigma \lesssim 2.465 \text{ TeV}$, as inferred from Fig. 2. As working benchmark values, we will thus set the

masses of the three generations¹⁰ of m_{Σ^i} as 2.45, 3.5 and 4.5 TeV. By construction, the other Z_2 -odd particle, h_2 , must be necessarily heavier than Σ^1 ; in order to comply with the hierarchy of the Z_2 -odd spectrum, we choose $m_{h_2} \sim 2.6$ TeV. Notice that h_1 is not subject to any DM-related arguments; its mass is not related to that of the LZoP, nor to m_{h_2} , and can in principle vary in the TeV range.

The chosen (illustrative) benchmark values of the scalar leptoquarks and fermion triplets are in agreement with the current limits established by negative collider searches; we refer to [57, 75] for a detailed discussion. We nevertheless highlight here a few important points, and current experimental bounds. Both leptoquarks can be pair produced via strong interactions $pp \rightarrow h_{1(2)}h_{1(2)}$; each of the Z_2 -even h_1 can subsequently decay into quark-lepton pairs (either neutrino or charged lepton). Searches for dilepton+dijet signals have been carried by the ATLAS and CMS collaborations: for the 13 TeV run data, and considering decays into ue and $c\mu$, ATLAS has set lower bounds on leptoquark masses of $\gtrsim 1100$ GeV (900 GeV), respectively assuming 100% (50%) branching fractions [149]; mass limits on leptoquarks decaying to $b\tau$ have been established by CMS, which has reported bounds $\gtrsim 850$ GeV (550 GeV) assuming 100% (50%) branching fractions [150]. The Z_2 -odd h_2 can decay into Σ and a down type quark; the decay mode associated with the neutral component of the triplet leads to a dijet + \cancel{E}_T signal (common to several supersymmetry search channels). Preliminary bounds on the mass of h_2 can thus be inferred from current squark mass limits: about 1.3 TeV for first generation scalar down quarks [151] and 800 GeV for third generation sbottoms [152].

A survey of the previous sections dedicated to neutrino masses and flavour observables reveals that the Yukawa couplings of the leptoquark h_1 to matter are at the core of the distinct observables so far discussed: on the one hand, y is responsible for saturating the B -meson anomalies and accounting for ν -oscillation data (recall that \tilde{y} can be inferred from y using a modified Casas-Ibarra parametrisation, see Eq. (22)); on the other, its different entries are severely constrained by the strong bounds arising either from negative searches or apparent SM-compatibility of a vast array of flavour observables. Our first goal will thus be to identify the most minimal flavour textures that can comply with the points listed above.

8.1 Towards a parametrisation of the scalar leptoquark Yukawa couplings

Similarly to what occurs with the quark and lepton Yukawa couplings in the SM, the new couplings are associated with numerous degrees of freedom (being complex, y contains 18 free parameters) which, in the absence of a full theory of flavour, can only be moderately constrained by data.

A possible approach to circumvent the latter problem relies in extending the symmetry group to include flavour symmetries, which can effectively reduce the number of free parameters. To this end, there have been attempts to obtain hierarchical leptoquark patterns by embedding the extended particle content in a Froggatt-Nielsen framework, which can also explain the fermion mass hierarchies as well as the CKM mixing pattern [153]. The Froggatt-Nielsen (FN) mechanism is usually implemented via a $U(1)$ symmetry¹¹ and a singlet scalar, non-trivially charged under the $U(1)_{\text{FN}}$. The singlet scalar then acquires a vacuum expectation value v_{FN} at some high scale Λ_{FN} , resulting in a suppression of the non-renormalisable Yukawa interactions by a factor $(v_{\text{FN}}/\Lambda_{\text{FN}})^n$,

¹⁰Note that a priori there is no reason to assume a hierarchical structure for m_{Σ} ; however, in the case of a degenerate spectrum, the Boltzmann equations relevant for calculating the dark matter relic abundance must take into account all three generations. Still, all other (qualitative) conclusions would remain valid in such a case.

¹¹Alternatively, a discrete Z_N symmetry which becomes nearly continuous in the limit of large N , has also been considered, see for example [154–157].

where n is the sum of the fermion $U(1)_{\text{FN}}$ charges [70]. Alternatively, a weakly broken $U(2)^5$ flavour symmetry has also been proposed in the context of possible interpretations of the B -decay anomalies [158].

A systematic and comprehensive study of the allowed textures for the leptoquark couplings, relying on symmetry-inspired flavour constructions, clearly lies beyond the scope of the analysis; here, we will adopt a phenomenological approach, and identify possible textures for the new Yukawa couplings from the requirements of explaining the B -meson anomalies while complying with all available experimental bounds. As a starting point (inspired by generic FN-like flavour patterns), we consider generic parametrisations of y in terms of powers of a small parameter ϵ (taken to be positive and real), with each entry¹² weighed by an $\mathcal{O}(1)$ real coefficient a_{ij} :

$$y_{ij} = a_{ij} \odot \epsilon^{n_{ij}}, \quad (86)$$

with \odot denoting that there is no summation implied over i, j .

As a first step, we set the individual coefficients $a_{ij} = 1$, and use the requirement of saturating the $R_{K^{(*)}}$ tensions to infer the size of the parameter ϵ : in Section 5 we have seen that at the leading order, the explanation of the $R_{K^{(*)}}$ anomalies constrains combinations of the quark-“muon” couplings y_{22} and y_{32} (further depending on inverse powers of the h_1 leptoquark mass). For a benchmark value of $m_{h_1} \sim 1.5$ TeV, one is led to the following relation

$$y_{22} y_{32} \approx 2.1555 \times 10^{-3} \sim \epsilon^{n_{22}+n_{32}} \rightarrow \epsilon^4 \sim 2.1555 \times 10^{-3} \Leftrightarrow \epsilon \approx 0.215, \quad (87)$$

in which we have elected $n_{22} + n_{32} = 4$ as a natural choice (so that $\epsilon \sim \mathcal{O}(1)$).

Following the above, and having fixed $\epsilon \approx 0.215$ (notice that this value reflects the choice of m_{h_1}), we express the most general texture written in terms of the parameter ϵ and positive integers $n_{ij} \geq 1$ with $i, j = 1, 2, 3$:

$$y \sim \begin{pmatrix} \epsilon^{n_{11}} & \epsilon^{n_{12}} & \epsilon^{n_{13}} \\ \epsilon^{n_{21}} & \epsilon^{n_{22}} & \epsilon^{n_{23}} \\ \epsilon^{n_{31}} & \epsilon^{n_{32}} & \epsilon^{n_{33}} \end{pmatrix}, \quad (88)$$

subject to the constraint $n_{22} + n_{32} = 4$ to explain the $R_{K^{(*)}}$ anomalies. The experimental bounds on rare meson and charged lepton decays can now be used to identify generic textures¹³ for y which are compatible with observation.

As can be inferred from the analytical expressions presented in Sections 6 and 7, the Yukawa couplings of h_1 to the first two generations of quarks are stringently constrained from rare meson decays; likewise, its couplings to the first generations of leptons are expected to be limited by cLFV transitions in the $\mu - e$ sector. A numerical scan of all possible textures (i.e., thorough tests on the viability of each $y(n_{ij})$ - cf. Eq. (88), for fixed values of ϵ and m_{h_1} and with $n_{22} + n_{32} = 4$) has shown that the most constraining observables turn out to be the rare decay $K^+ \rightarrow \pi^+ \nu \bar{\nu}$ and, on the lepton sector, $\mu - e$ conversion in nuclei and the radiative $\mu \rightarrow e \gamma$ decay.

The numerical study has further allowed to identify generic classes of representative textures which are in agreement with the B -meson anomalies as well as all leptonic and mesonic processes taken into account (for the above mentioned (ϵ, m_{h_1}) benchmark): $\mu \rightarrow e \gamma$, $\tau \rightarrow e \gamma$, $\tau \rightarrow \mu \gamma$,

¹²Notice that the Yukawa matrix y is a priori a complex matrix in flavour space; however, for simplicity, we will only consider real values both for ϵ and for a_{ij} .

¹³Another approach to constrain y would be to consider minimal textures exhibiting vanishing entries (“texture zeroes”) in a given weak basis; however, in the absence of an underlying symmetry, we prefer to consider the most general pattern for y_{ij} .

$\mu \rightarrow 3e$, $\tau \rightarrow 3\mu$, $\mu - e$ conversion, and $K^+(K_L) \rightarrow \pi\nu\bar{\nu}$, $B \rightarrow K^*\nu\bar{\nu}$, $B_s^0 - \bar{B}_s^0$ oscillations¹⁴, as well as the cLFV decays $B_s \rightarrow \mu e$ and $K_L \rightarrow \mu e$.

The three classes of textures are identified by the specific realisation of (n_{22}, n_{32}) : (3, 1) - type I; (2, 2) - type II; (1, 3) - type III. For each class, the allowed textures are presented in Table 5.

	Type I	Type II	Type III
y	$\begin{pmatrix} \times & \times & \times \\ \times & \epsilon^3 & \times \\ \times & \epsilon & \times \end{pmatrix}$	$\begin{pmatrix} \times & \times & \times \\ \times & \epsilon^2 & \times \\ \times & \epsilon^2 & \times \end{pmatrix}$	$\begin{pmatrix} \times & \times & \times \\ \times & \epsilon & \times \\ \times & \epsilon^3 & \times \end{pmatrix}$
Generic allowed textures	$\begin{pmatrix} \epsilon^4 & \epsilon^{\geq 5} & \epsilon^{\geq 2} \\ \epsilon^{\geq 3} & \epsilon^3 & \epsilon^{\geq 4} \\ \epsilon^{\geq 4} & \epsilon & \epsilon^{\geq 1} \end{pmatrix}$	$\begin{pmatrix} \epsilon^6 & \epsilon^{\geq 4} & \epsilon^{\geq 3} \\ \epsilon^{\geq 5} & \epsilon^2 & \epsilon^{\geq 3} \\ \epsilon^{\geq 3} & \epsilon^2 & \epsilon^{\geq 1} \end{pmatrix}$	$\begin{pmatrix} \epsilon^5 & \epsilon^{\geq 5} & \epsilon^{\geq 4} \\ \epsilon^4 & \epsilon & \epsilon^{\geq 2} \\ \epsilon^{\geq 4} & \epsilon^3 & \epsilon^{\geq 1} \end{pmatrix}$

Table 5: Classes of textures for the y couplings complying with the constraint $n_{22} + n_{32} = 4$: type I, II and III. For a small parameter ($\epsilon \sim 0.215$), the second row displays the generic allowed textures in terms of powers of ϵ , consistent with the current experimental bounds on the leptonic processes $\ell \rightarrow \ell'\gamma$, $\ell \rightarrow 3\ell'$, $\mu - e$ conversion in nuclei, $K^+(K_L) \rightarrow \pi^+(\pi^0)\nu\bar{\nu}$, $B \rightarrow K^*\nu\bar{\nu}$, $B_s^0 - \bar{B}_s^0$ oscillation and $B_s \rightarrow \mu e$, $K_L \rightarrow \mu e$.

For each of the classes identified, we have chosen an illustrative case (setting n_{ij} in agreement with Table 5), and we have evaluated the associated contributions to the different leptonic and mesonic observables mentioned above. The information is summarised in Table 6. We do not include here bounds from the neutral meson-antimeson oscillations since they are considerably less constraining than the meson decay processes involving the same set of leptoquark couplings.

Figure 4 graphically summarises the information given in Table 6: for each type of texture, we display the associated predictions for $\mu \rightarrow e\gamma$, $\tau \rightarrow \mu\gamma$, $\tau \rightarrow e\gamma$, $\mu \rightarrow 3e$, $\tau \rightarrow 3\mu$, $\mu - e$ conversion, $K^+(K_L) \rightarrow \pi^+(\pi^0)\nu\bar{\nu}$, $R_{K^{(*)}}^{\nu\nu}$ as well as $B_s \rightarrow \mu e$ and $K_L \rightarrow \mu e$. For each process we include the current experimental bounds and future sensitivities, and when applicable, the SM predictions.

Before proceeding, we briefly comment on the other LFUV observables discussed in Section 5.2. The present leptoquark construction leads to SM-like predictions to the distinct $R_{D^{(*)}}$ ratios (independently of the texture type and/or mass regime for the exchanged pseudoscalar). If on the one hand this means that, once the distinct experimental constraints have been taken into account, the muon to electron ratios $R_{D^{(*)}}^{\mu/e}$ are consistent with experimental measurements, on the other hand it also implies that the current experimental measurement of $R_{D^{(*)}}$ (tau to muon ratio, exhibiting a significant deviation from SM predictions) cannot be accounted for. Should the latter $R_{D^{(*)}}$ discrepancy be confirmed in the future, then the present leptoquark construction will be ruled out, at least in this minimal version.

8.2 Constraining the leptoquark parameter space

The previously chosen textures, as well as the numerical results (both for the ϵ parameter and for the contributions to the distinct observables) were obtained for a benchmark value of the h_1

¹⁴In the subsequent discussion we do not include constraints from $K^0 - \bar{K}^0$ mixing, as the latter was found to provide weaker constraints than those arising from $K \rightarrow \pi\nu\bar{\nu}$ decays.

	Type I	Type II	Type III
y example	$\begin{pmatrix} \epsilon^4 & \epsilon^5 & \epsilon^2 \\ \epsilon^3 & \epsilon^3 & \epsilon^4 \\ \epsilon^4 & \epsilon & \epsilon \end{pmatrix}$	$\begin{pmatrix} \epsilon^6 & \epsilon^4 & \epsilon^3 \\ \epsilon^5 & \epsilon^2 & \epsilon^3 \\ \epsilon^3 & \epsilon^2 & \epsilon \end{pmatrix}$	$\begin{pmatrix} \epsilon^5 & \epsilon^5 & \epsilon^4 \\ \epsilon^4 & \epsilon & \epsilon^2 \\ \epsilon^4 & \epsilon^3 & \epsilon \end{pmatrix}$
BR($\mu \rightarrow e\gamma$)	1.21×10^{-13}	8.99×10^{-14}	8.31×10^{-14}
BR($\tau \rightarrow \mu\gamma$)	1.47×10^{-10}	7.45×10^{-12}	9.46×10^{-12}
BR($\tau \rightarrow e\gamma$)	2.31×10^{-14}	3.17×10^{-13}	2.14×10^{-14}
BR($\mu \rightarrow 3e$)	2.73×10^{-13}	2.02×10^{-13}	2.02×10^{-13}
BR($\tau \rightarrow 3\mu$)	1.92×10^{-9}	9.49×10^{-11}	1.30×10^{-10}
BR($\tau \rightarrow 3e$)	2.93×10^{-13}	4.01×10^{-12}	2.73×10^{-13}
CR($\mu - e, N$)	1.81×10^{-13}	2.75×10^{-14}	1.61×10^{-13}
BR($K^+ \rightarrow \pi^+ \nu \bar{\nu}$)	1.32×10^{-10}	1.21×10^{-10}	1.22×10^{-10}
BR($K_L \rightarrow \pi^0 \nu \bar{\nu}$)	3.25×10^{-11}	3.10×10^{-11}	3.10×10^{-11}
$R_{K^{(*)}}^{\nu\nu}$	1.04	1.08	1.53
BR($K_L \rightarrow \mu e$)	1.96×10^{-13}	9.06×10^{-15}	9.06×10^{-15}
BR($B_s \rightarrow \mu e$)	3.13×10^{-15}	1.47×10^{-12}	1.47×10^{-12}

Table 6: Contributions to distinct observables associated with illustrative examples of each of the texture classes given in Table 5 (viable for the benchmark choice $(\epsilon, m_{h_1}) = (0.215, 1.5 \text{ TeV})$).

leptoquark mass, $m_{h_1} = 1.5 \text{ TeV}$. The natural question to address is how the viability of the model is impacted by different choices of its parameters, in particular the entries of the y couplings and m_{h_1} .

To explain the $R_{K^{(*)}}$ anomalies, the BSM construction must comply with the conditions given in Section 5.1, in particular with the interval for the $C_{9,\text{NP}}^{ee,\mu\mu}$ couplings given in Eq. (39); this can also be written as a condition on the ratio of the relevant Yukawa couplings to the h_1 leptoquark mass, $0.64 \times 10^{-3} \lesssim \frac{\text{Re}[y_{b\mu} y_{s\mu}^* - y_{be} y_{se}^*]}{(m_{h_1}/1 \text{ TeV})^2} \lesssim 1.12 \times 10^{-3}$.

Varying the mass of the h_1 leptoquark over a wide interval - in agreement with LHC direct search bounds - leads to new ranges for the relevant entries of the Yukawa couplings y_{ij} (and thus new values for ϵ). Since for increasing values of m_{h_1} saturating the $R_{K^{(*)}}$ anomalies calls for larger $y_{22,32}$ - and hence for larger ϵ -, bounds on other observables are expected to become more severe, leading to the exclusion of a given realisation. This is displayed on the distinct panels of Fig. 5: the coloured regions denote the contributions for a given observable arising from varying ϵ (i.e., y_{ij}) in the $R_{K^{(*)}}$ favoured interval given above. Light (dark) regions correspond to allowed (excluded) regimes in view of current experimental bounds.

Leading to Fig. 5 we have elected to plot only the most constraining observables: BR($\mu \rightarrow e\gamma$), BR($\mu \rightarrow 3e$), CR($\mu - e, \text{Au}$) and BR($K^+ \rightarrow \pi^+ \nu \bar{\nu}$). Concerning textures of type I and II, one can verify that CR($\mu - e, \text{Au}$) precludes values of the leptoquark mass respectively larger than $m_{h_1} \gtrsim 1.8 \text{ TeV}$ and 3.4 TeV (for ϵ_{max}) and $m_{h_1} \gtrsim 3 \text{ TeV}$ and 4.2 TeV (for ϵ_{min}). (Notice that for texture II $\mu \rightarrow 3e$ is almost as constraining as $\mu - e$ conversion in nuclei.) For type III textures, one finds two intervals for m_{h_1} : $[1.75 \text{ TeV}, 2.75 \text{ TeV}]$ and $[8 \text{ TeV}, 11.4 \text{ TeV}]$ (the lower and upper

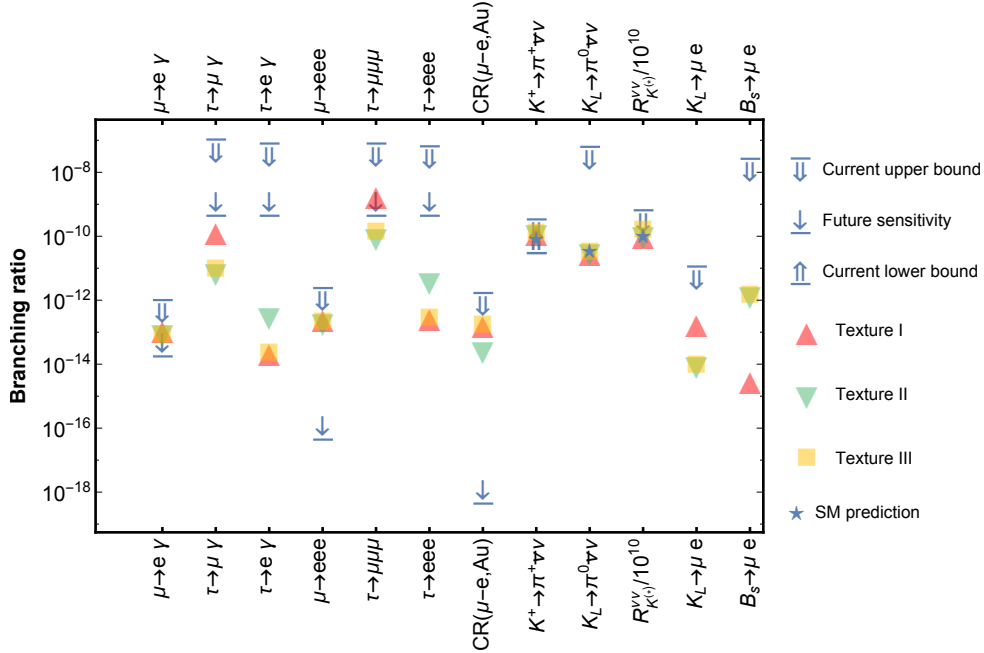


Figure 4: Contributions to several leptonic and mesonic observables associated with the three textures I, II, and III for the benchmark choice $(\epsilon, m_{h_1}) = (0.215, 1.5 \text{ TeV})$: $\mu \rightarrow e\gamma$, $\tau \rightarrow \mu\gamma$, $\tau \rightarrow e\gamma$, $\mu \rightarrow 3e$, $\tau \rightarrow 3\mu$, $\mu - e$ conversion, $K^+(K_L) \rightarrow \pi^+(\pi^0)\nu\bar{\nu}$, $R_{K^{(*)}}^{\nu\nu}/10^{10}$, $B_s \rightarrow \mu e$, and $K_L \rightarrow \mu e$. The relevant experimental bounds (and future sensitivities), as well as SM predictions (when appropriate), are also displayed.

bounds obtained in association with the maximal and minimal values of ϵ).

Despite being manifest in all panels, the “kinks” associated with the contributions to $\text{CR}(\mu - e, \text{Au})$ are particularly apparent for type III textures¹⁵. The behaviour has been well identified in the literature (see, e.g. [159]), and stems from having a localised cancellation of opposite sign up- and down-type quark contributions to the conversion rate (due to different charge and weak isospin).

At this point, it is important to recall that the proposed parametrisation for y , as given in Eq. (86), allows each element to be weighed by a real coefficient a_{ij} , $\mathcal{O}(1)$. In order to understand how generic perturbations of the unconstrained entries of y affect the phenomenological viability of the model, we have thus taken a type I texture for y , and varied one a_{ij} at a time¹⁶ in the range $[0.4, 1.6]$ (with a step size of 0.1). Although not explicitly displayed here, the numerical studies revealed that $\mu \rightarrow e\gamma$ and $\mu \rightarrow 3e$ are predominantly sensitive to y_{31} (a_{31}), with a mild secondary dependence on y_{21} (a_{21}); likewise, $\tau \rightarrow \mu\gamma$ and $\tau \rightarrow 3\mu$ are controlled by y_{33} (a_{33}); $\tau \rightarrow e\gamma$ and $\tau \rightarrow 3e$ are sensitive to variations from both y_{31} and y_{33} . Finally, $K^+ \rightarrow \pi^+\nu\bar{\nu}$ exhibits a significant dependence on y_{13} (a_{13}), y_{21} (a_{21}) and y_{23} (a_{23}). As a general qualitative statement, for all the radiative and 3-body decays mentioned above, the variation of the a_{ij} coefficients in

¹⁵For this reason we have preferred to display several lines associated with values of ϵ , which is varied with a 5×10^{-5} step.

¹⁶We fix $y_{22,32}$ to ensure that $R_{K^{(*)}}$ remains accounted for, hence $a_{22,32} = 1$.

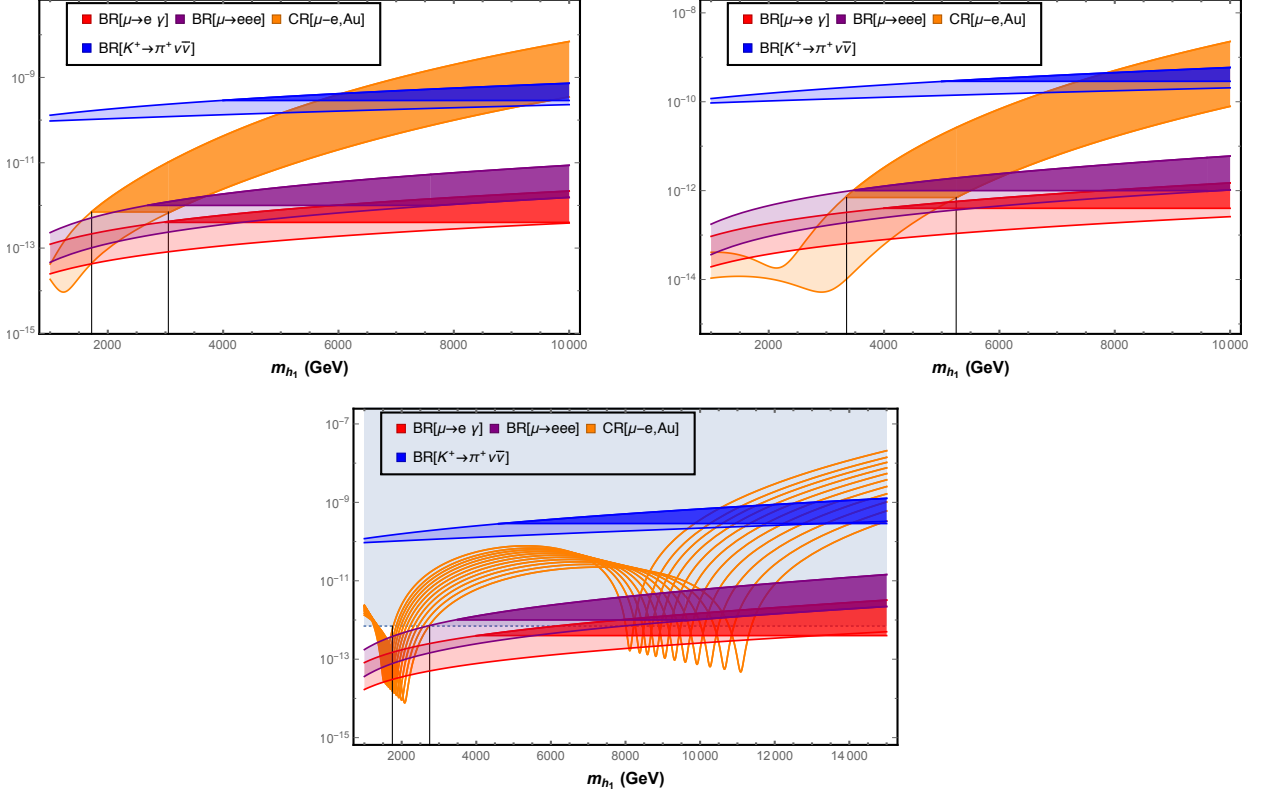


Figure 5: Contributions to $\text{BR}(\mu \rightarrow e\gamma)$, $\text{BR}(\mu \rightarrow 3e)$, $\text{CR}(\mu - e, \text{Au})$ and $\text{BR}(K^+ \rightarrow \pi^+ \nu \bar{\nu})$ as a function of the h_1 leptoquark mass m_{h_1} , for type I, II and III textures of y (respectively from left to right, top to bottom), complying with the current interval for $R_{K^{(*)}}$. Light (solid) surfaces denote currently allowed (excluded) regimes due to the violation of the associated experimental bound.

the interval $[0.4, 1.6]$ leads to a variation of about one order of magnitude in the prediction for the observable. Occurring at the tree level, the neutrinoless $\mu - e$ conversion strongly depends on y_{11} (a_{11}), y_{12} (a_{12}), and y_{21} (a_{21}) - the dominant element depending to a certain extent on the leptoquark mass regime.

The same study can be carried for type II and III textures, with the results reflecting the relative $\epsilon^{n_{ij}}$ dependence.

8.3 Final constraints from neutrino oscillation data

The requirements of having a viable DM candidate, and of accounting for the $R_K^{(*)}$ anomalies while complying with all available data on meson and lepton rare decays and transitions have allowed to identify viable flavour textures for the y leptoquark Yukawa couplings, as well as mass regimes for the new states.

As mentioned in Section 3, once the flavour structure of y has been fixed (be it from theoretical arguments or, as in the present case, from a comprehensive phenomenological analysis), the modified Casas-Ibarra parametrisation of Eq. (22) readily allows to determine \tilde{y} , while complying with current neutrino oscillation data. As a final step in our study, we thus consider the three

textures already discussed in the previous section, and for each one we vary the n_{ij} powers of ϵ in agreement with the ranges given in Table 5, as well as the associated a_{ij} prefactors (in the range [0.4,1.6]). The h_1 leptoquark mass is, for simplicity, set to the benchmark value of 1.5 TeV (although the results here discussed qualitatively hold for other choices - in agreement with the discussion of the previous subsection).

Concerning neutrino data, we use the best-fit values from the global oscillation analysis of [160], taking a normal ordering for the neutrino spectrum, with the lightest neutrino mass taken in the range [10⁻⁸ eV, 0.001 eV]. As already mentioned, we take the right-handed triplet masses to be $m_\Sigma=2.45, 3.5$ and 4.5 TeV. The remaining degrees of freedom in the modified Casas-Ibarra parametrisation are randomly sampled from the following intervals: $[0, 2\pi]$ for the phases, and $[-4\pi, 4\pi]$ for the angles; one further has $\lambda_h \lesssim 4\pi$ (see Eq. (8)).

Each of the thus obtained couplings (y and \tilde{y}) are again subject to the various flavour constraints previously discussed; moreover, each entry of the couplings must comply with perturbativity requirements, $|y(\tilde{y})| \lesssim 4\pi$.

In order to illustrate our findings, we display in Fig. 6 the results of the scan, for the three types of textures. Since neutrinoless conversion in nuclei and the $K^+ \rightarrow \pi^+ \nu \bar{\nu}$ decay are the most constraining observables, we display the corresponding predictions of the randomly sampled textures in the plane spanned by the latter two observables; the colour code distinguishes between perturbative and non-perturbative entries of the y and \tilde{y} couplings.

As is manifest from inspection of Fig. 6, accommodating ν -oscillation data from type I textures for the leptoquark y couplings, in agreement with experimental data, and for perturbative \tilde{y} does not excessively constrain the remaining degrees of freedom. Even though perturbative regimes for \tilde{y} are more likely to be associated with large values of $\text{BR}(K^+ \rightarrow \pi^+ \nu \bar{\nu})$, one can easily find regimes which are phenomenologically allowed. Notice however that a near-future improvement in the associated experimental sensitivities (for instance $\text{CR}(\mu - e, \text{Al}) \sim 10^{-15}$, and $\text{BR}(K^+ \rightarrow \pi^+ \nu \bar{\nu}) \sim 10^{-10}$) should allow to probe the present leptoquark construction (and possibly falsify it).

For type II textures, the associated panel of Fig. 6 reveals that perturbative \tilde{y} couplings are far harder to accommodate, especially due to the excessive contributions to $\text{CR}(\mu - e, \text{Au})$. Finally, notice that only a tiny subset of the sampled type III textures is in agreement with flavour observables, and no sub-region of the latter leads to perturbative \tilde{y} . One thus concludes that type III textures (despite being marginally compatible with all the quark and lepton observables here discussed) do not lead to a satisfactory leptoquark construction.

We have also explored the possibility of having a distinct ordering (inverted) for the light neutrino spectrum: in what concerns type I textures, we found no significant changes, so that in fact both orderings can be easily accommodated; in the case of type II textures for y (which do allow to accommodate oscillation data for a normal ordering) we failed to find viable solutions for an inverted ordering; finally, type III textures remain unable to account for oscillation data with perturbative values of the couplings even in the case of a inverted ordering of the neutrino spectrum.

Before moving to our final remarks, it is worth mentioning that it would have been theoretically appealing to have FN-inspired textures for both y and \tilde{y} couplings; as can be indirectly inferred from the above discussion, we did not succeed in finding phenomenologically viable \tilde{y} couplings with textures mirroring those of y .

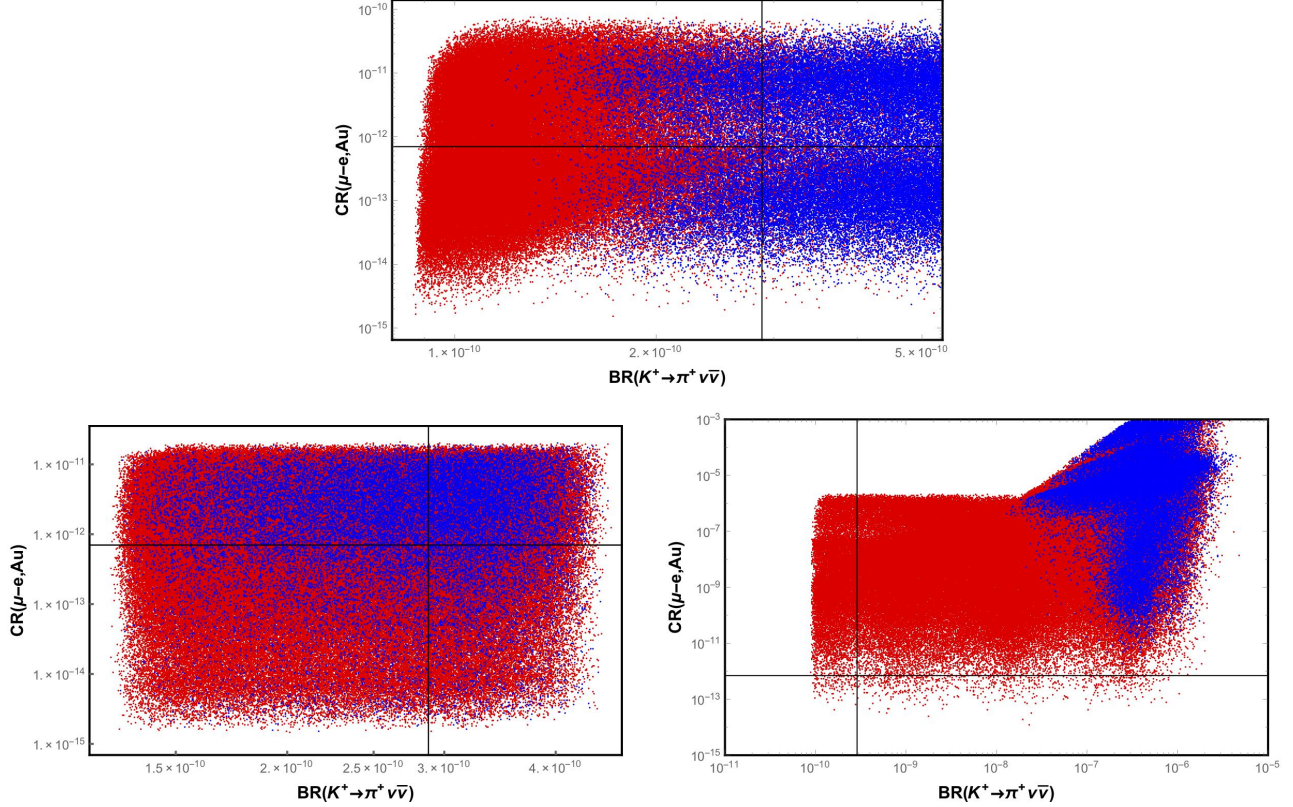


Figure 6: Predictions for $\text{CR}(\mu - e, N)$ and $\text{BR}(K^+ \rightarrow \pi^+ \nu \bar{\nu})$ associated with randomly sampled y and \tilde{y} (see text), for type I, II and III textures (top to bottom, left to right). The horizontal/vertical lines denote the current experimental bounds, and the colour code identifies perturbative (blue) or non-perturbative (red) regimes of \tilde{y} .

9 Concluding remarks

In this work we have carried a comprehensive phenomenological study of a SM extension via two scalar leptoquarks $h_{1,2}$ and three generations of triplet neutrinos Σ_R^i , further reinforcing the SM gauge group via a discrete Z_2 symmetry under which h_2 and Σ_R^i are odd (all other fields being even).

The present New Physics construction aims at simultaneously addressing two long-standing SM observational problems - neutrino mass generation, and a viable dark matter candidate - while further offering a solution to the currently reported anomalies in B meson decays, $R_{K^{(*)}}$.

The Z_2 symmetry ensures the stability of the LZoP, rendering the neutral component of the lightest Σ_R a viable cold dark matter candidate for well defined intervals of its mass. In the absence of a full theory of flavour, we have identified several classes of flavour textures for the h_1 leptoquark Yukawa couplings which succeed in saturating the $R_{K^{(*)}}$ anomalies. These textures (loosely based on Froggatt-Nielsen inspired ansätze) were subjected to a vast array of flavour conserving and flavour violating observables (including meson decays, neutral meson oscillations and cLFV decays), which allowed to infer stringent constraints on the h_1 leptoquark mass and couplings. Contrary to previous claims in the literature, our findings suggest that the strongest constraints on these leptoquark extensions do arise from cLFV $\mu - e$ conversion in nuclei, and from

the rare $K^+ \rightarrow \pi^+ \nu \bar{\nu}$ decays. Furthermore, we also verified that numerous ansätze (identified as promising ones for leptoquarks couplings, see e.g. [74, 75]) were in fact phenomenologically disfavoured by several of the here considered observables.

It is important to emphasise that the constraints on leptoquark couplings arising from flavour observables are not intrinsic (nor peculiar) to the leptoquark realisation here considered; in fact these are valid for any SM extension via scalar triplet leptoquarks.

The present BSM realisation leads to a scenario in which neutrino masses are radiatively generated (at the three-loop level, from the exchange of leptoquarks, down-type quarks and lepton triplets, see Fig. 1). Neutrino oscillation data can be accounted for by means of a modified Casas-Ibarra parametrisation: avoiding non-perturbative regimes for the Yukawa couplings, y and \tilde{y} , establishes the final constraints on the parameter space of the model.

The inclusion of Majorana states opens the door to lepton number violating processes; the radiatively induced masses for the light (left-handed) neutrinos are one such example. The new interactions and couplings further allow for additional sources of CP violation. It is thus only natural to envisage the possibility of accounting for the baryon asymmetry of the universe. In the present realisation, one can have tree-level processes which are lepton number violating: one such example can be obtained from the neutrino mass (loop) diagrams - see Fig. 1 -, by “cutting” the inner fermion propagators. This would lead to tree-level LNV decays of the heavier neutral $\Sigma_R^{2,0}$ into, for instance, $\Sigma_R^{1,0} + \bar{d} + \bar{d} + d\nu_L + d\nu_L$ (which could have CP violating interferences with higher order diagrams). However, these appear to be heavily suppressed processes and, in the absence of a detailed evaluation, it remains unclear whether one could indeed generate a significant lepton asymmetry. In addition, Σ_R decoupling would be required to occur above the EW phase transition to have an efficient conversion into a baryon asymmetry.

In summary, and following a thorough study of an extensive array of observables, we have proposed realisations of a SM scalar leptoquark extension capable of accommodating neutrino oscillation data, a viable DM candidate, and saturating the observed discrepancies for $R_{K^{(*)}}$. We notice that the present construction cannot account for the tensions in $R_{D^{(*)}}$, nor for the discrepancy between observation and SM prediction in what concerns the muon anomalous magnetic moment. Should the latter persist, then the candidate model here studied will have to be extended, or then embedded in a larger framework [62].

In the near future, a number of high-intensity experiments will put the present leptoquark construction to the test, in particular several cLFV-dedicated facilities (searches for radiative and three-body muon decays, in addition to neutrinoless conversion in nuclei) and a possible measurement of the rare decay $K^+ \rightarrow \pi^+ \nu \bar{\nu}$. Hopefully, positive signals or new stringent bounds emerging from negative searches, will allow to further constrain the model’s parameter space, or possibly disfavour it as a candidate New Physics model.

Acknowledgements

We are grateful to Damir Bečirević and Gudrun Hiller for valuable discussions and suggestions. C.H., J.O. and A.M.T. acknowledge support within the framework of the European Union’s Horizon 2020 research and innovation programme under the Marie Skłodowska-Curie grant agreements No 690575 and No 674896.

References

- [1] C. Patrignani *et al.* [Particle Data Group], *Chin. Phys. C* **40**, no. 10, 100001 (2016).
- [2] G. Hiller and F. Kruger, *Phys. Rev. D* **69**, 074020 (2004) [hep-ph/0310219].
- [3] R. Aaij *et al.* [LHCb Collaboration], *Phys. Rev. Lett.* **113**, 151601 (2014) [arXiv:1406.6482 [hep-ex]].
- [4] M. Bordone, G. Isidori and A. Pattori, *Eur. Phys. J. C* **76**, no. 8, 440 (2016) [arXiv:1605.07633 [hep-ph]].
- [5] B. Capdevila, A. Crivellin, S. Descotes-Genon, J. Matias and J. Virto, *JHEP* **1801**, 093 (2018) [arXiv:1704.05340 [hep-ph]].
- [6] R. Aaij *et al.* [LHCb Collaboration], *JHEP* **1708**, 055 (2017) [arXiv:1705.05802 [hep-ex]].
- [7] <http://www.slac.stanford.edu/xorg/hflav/semi/fpcp17/RDRDs.html>
- [8] J. P. Lees *et al.* [BaBar Collaboration], *Phys. Rev. Lett.* **109**, 101802 (2012) [arXiv:1205.5442 [hep-ex]].
- [9] J. P. Lees *et al.* [BaBar Collaboration], *Phys. Rev. D* **88**, no. 7, 072012 (2013) [arXiv:1303.0571 [hep-ex]].
- [10] M. Huschle *et al.* [Belle Collaboration], *Phys. Rev. D* **92**, no. 7, 072014 (2015) [arXiv:1507.03233 [hep-ex]].
- [11] I. Adachi *et al.* [Belle Collaboration], arXiv:0910.4301 [hep-ex].
- [12] A. Bozek *et al.* [Belle Collaboration], *Phys. Rev. D* **82**, 072005 (2010) [arXiv:1005.2302 [hep-ex]].
- [13] R. Aaij *et al.* [LHCb Collaboration], *Phys. Rev. Lett.* **115**, no. 11, 111803 (2015) Erratum: [*Phys. Rev. Lett.* **115**, no. 15, 159901 (2015)] [arXiv:1506.08614 [hep-ex]].
- [14] S. Hirose *et al.* [Belle Collaboration], *Phys. Rev. Lett.* **118**, no. 21, 211801 (2017) [arXiv:1612.00529 [hep-ex]].
- [15] D. Bigi and P. Gambino, *Phys. Rev. D* **94**, no. 9, 094008 (2016) [arXiv:1606.08030 [hep-ph]].
- [16] Y. Amhis *et al.* [HFLAV Collaboration], *Eur. Phys. J. C* **77**, no. 12, 895 (2017) [arXiv:1612.07233 [hep-ex]].
- [17] D. Bigi, P. Gambino and S. Schacht, *JHEP* **1711**, 061 (2017) [arXiv:1707.09509 [hep-ph]].
- [18] Z. Ligeti, M. Papucci and D. J. Robinson, *JHEP* **1701**, 083 (2017) [arXiv:1610.02045 [hep-ph]].
- [19] A. Crivellin, J. Fuentes-Martin, A. Greljo and G. Isidori, *Phys. Lett. B* **766**, 77 (2017) [arXiv:1611.02703 [hep-ph]].
- [20] B. Capdevila, S. Descotes-Genon, L. Hofer and J. Matias, *JHEP* **1704**, 016 (2017) [arXiv:1701.08672 [hep-ph]].
- [21] S. Wehle *et al.* [Belle Collaboration], *Phys. Rev. Lett.* **118**, no. 11, 111801 (2017) [arXiv:1612.05014 [hep-ex]].
- [22] A. Datta, M. Duraisamy and D. Ghosh, *Phys. Rev. D* **89**, no. 7, 071501 (2014) [arXiv:1310.1937 [hep-ph]].
- [23] D. Ghosh, M. Nardecchia and S. A. Renner, *JHEP* **1412**, 131 (2014) [arXiv:1408.4097 [hep-ph]].
- [24] S. L. Glashow, D. Guadagnoli and K. Lane, *Phys. Rev. Lett.* **114**, 091801 (2015) [arXiv:1411.0565 [hep-ph]].
- [25] B. Bhattacharya, A. Datta, D. London and S. Shivashankara, *Phys. Lett. B* **742**, 370 (2015) [arXiv:1412.7164 [hep-ph]].
- [26] M. Freytsis, Z. Ligeti and J. T. Ruderman, *Phys. Rev. D* **92**, no. 5, 054018 (2015) [arXiv:1506.08896 [hep-ph]].
- [27] D. Bardhan, P. Byakti and D. Ghosh, *JHEP* **1701**, 125 (2017) [arXiv:1610.03038 [hep-ph]].

- [28] D. Ghosh, *Eur. Phys. J. C* **77**, no. 10, 694 (2017) [arXiv:1704.06240 [hep-ph]].
- [29] M. Ciuchini, A. M. Coutinho, M. Fedele, E. Franco, A. Paul, L. Silvestrini and M. Valli, *Eur. Phys. J. C* **77**, no. 10, 688 (2017) [arXiv:1704.05447 [hep-ph]].
- [30] D. Choudhury, A. Kundu, R. Mandal and R. Sinha, *Phys. Rev. Lett.* **119**, no. 15, 151801 (2017) [arXiv:1706.08437 [hep-ph]].
- [31] D. Choudhury, A. Kundu, R. Mandal and R. Sinha, arXiv:1712.01593 [hep-ph].
- [32] W. Altmannshofer, S. Gori, M. Pospelov and I. Yavin, *Phys. Rev. D* **89**, 095033 (2014) [arXiv:1403.1269 [hep-ph]].
- [33] A. Crivellin, G. D'Ambrosio and J. Heeck, *Phys. Rev. Lett.* **114**, 151801 (2015) [arXiv:1501.00993 [hep-ph]].
- [34] A. Crivellin, G. D'Ambrosio and J. Heeck, *Phys. Rev. D* **91**, no. 7, 075006 (2015) [arXiv:1503.03477 [hep-ph]].
- [35] D. Aristizabal Sierra, F. Staub and A. Vicente, *Phys. Rev. D* **92**, no. 1, 015001 (2015) [arXiv:1503.06077 [hep-ph]].
- [36] A. Crivellin, L. Hofer, J. Matias, U. Nierste, S. Pokorski and J. Rosiek, *Phys. Rev. D* **92**, no. 5, 054013 (2015) [arXiv:1504.07928 [hep-ph]].
- [37] A. Celis, J. Fuentes-Martin, M. Jung and H. Serodio, *Phys. Rev. D* **92**, no. 1, 015007 (2015) [arXiv:1505.03079 [hep-ph]].
- [38] D. Bhatia, S. Chakraborty and A. Dighe, *JHEP* **1703**, 117 (2017) [arXiv:1701.05825 [hep-ph]].
- [39] J. F. Kamenik, Y. Soreq and J. Zupan, *Phys. Rev. D* **97**, no. 3, 035002 (2018) [arXiv:1704.06005 [hep-ph]].
- [40] J. E. Camargo-Molina, A. Celis and D. A. Faroughy, arXiv:1805.04917 [hep-ph].
- [41] G. Hiller and M. Schmaltz, *Phys. Rev. D* **90**, 054014 (2014) [arXiv:1408.1627 [hep-ph]].
- [42] B. Gripaios, M. Nardecchia and S. A. Renner, *JHEP* **1505**, 006 (2015) [arXiv:1412.1791 [hep-ph]].
- [43] S. Sahoo and R. Mohanta, *Phys. Rev. D* **91**, no. 9, 094019 (2015) [arXiv:1501.05193 [hep-ph]].
- [44] I. de Medeiros Varzielas and G. Hiller, *JHEP* **1506**, 072 (2015) [arXiv:1503.01084 [hep-ph]].
- [45] R. Alonso, B. Grinstein and J. Martin Camalich, *JHEP* **1510**, 184 (2015) [arXiv:1505.05164 [hep-ph]].
- [46] M. Bauer and M. Neubert, *Phys. Rev. Lett.* **116**, no. 14, 141802 (2016) [arXiv:1511.01900 [hep-ph]].
- [47] C. Hati, G. Kumar and N. Mahajan, *JHEP* **1601**, 117 (2016) [arXiv:1511.03290 [hep-ph]].
- [48] S. Fajfer and N. Košnik, *Phys. Lett. B* **755**, 270 (2016) [arXiv:1511.06024 [hep-ph]].
- [49] D. Das, C. Hati, G. Kumar and N. Mahajan, *Phys. Rev. D* **94**, 055034 (2016) [arXiv:1605.06313 [hep-ph]].
- [50] D. Bečirević, S. Fajfer, N. Kosnik and O. Sumensari, *Phys. Rev. D* **94**, no. 11, 115021 (2016) [arXiv:1608.08501 [hep-ph]].
- [51] S. Sahoo, R. Mohanta and A. K. Giri, *Phys. Rev. D* **95**, no. 3, 035027 (2017) [arXiv:1609.04367 [hep-ph]].
- [52] P. Cox, A. Kusenko, O. Sumensari and T. T. Yanagida, *JHEP* **1703**, 035 (2017) [arXiv:1612.03923 [hep-ph]].
- [53] A. Crivellin, D. Müller and T. Ota, *JHEP* **1709**, 040 (2017) [arXiv:1703.09226 [hep-ph]].
- [54] D. Bečirević and O. Sumensari, *JHEP* **1708**, 104 (2017) [arXiv:1704.05835 [hep-ph]].

- [55] Y. Cai, J. Gargalionis, M. A. Schmidt and R. R. Volkas, *JHEP* **1710**, 047 (2017) [arXiv:1704.05849 [hep-ph]].
- [56] D. Buttazzo, A. Greljo, G. Isidori and D. Marzocca, *JHEP* **1711**, 044 (2017) [arXiv:1706.07808 [hep-ph]].
- [57] I. Doršner, S. Fajfer, D. A. Faroughy and N. Košnik, *JHEP* **1710**, 188 (2017) [arXiv:1706.07779 [hep-ph]].
- [58] M. Blanke and A. Crivellin, arXiv:1801.07256 [hep-ph].
- [59] A. Greljo and B. A. Stefanek, *Phys. Lett. B* **782**, 131 (2018) [arXiv:1802.04274 [hep-ph]].
- [60] M. Bordone, C. Cornella, J. Fuentes-Martin and G. Isidori, arXiv:1805.09328 [hep-ph].
- [61] S. Sahoo and R. Mohanta, arXiv:1806.01048 [hep-ph].
- [62] D. Bečirević, I. Doršner, S. Fajfer, N. Košnik, D. A. Faroughy and O. Sumensari, arXiv:1806.05689 [hep-ph].
- [63] A. Greljo, G. Isidori and D. Marzocca, *JHEP* **1507**, 142 (2015) [arXiv:1506.01705 [hep-ph]].
- [64] P. Arnan, D. Bečirević, F. Mescia and O. Sumensari, *Eur. Phys. J. C* **77**, no. 11, 796 (2017) [arXiv:1703.03426 [hep-ph]].
- [65] L. S. Geng, B. Grinstein, S. Jäger, J. Martin Camalich, X. L. Ren and R. X. Shi, *Phys. Rev. D* **96**, no. 9, 093006 (2017) [arXiv:1704.05446 [hep-ph]].
- [66] W. Altmannshofer, P. S. Bhupal Dev and A. Soni, *Phys. Rev. D* **96**, no. 9, 095010 (2017) [arXiv:1704.06659 [hep-ph]].
- [67] D. Das, C. Hati, G. Kumar and N. Mahajan, *Phys. Rev. D* **96**, no. 9, 095033 (2017) [arXiv:1705.09188 [hep-ph]].
- [68] K. Earl and T. Gregoire, arXiv:1806.01343 [hep-ph].
- [69] Y. Cai, J. Herrero-García, M. A. Schmidt, A. Vicente and R. R. Volkas, *Front. in Phys.* **5**, 63 (2017) [arXiv:1706.08524 [hep-ph]].
- [70] F. F. Deppisch, S. Kulkarni, H. Päs and E. Schumacher, *Phys. Rev. D* **94**, no. 1, 013003 (2016) [arXiv:1603.07672 [hep-ph]].
- [71] A. Zee, *Nucl. Phys. B* **264**, 99 (1986).
- [72] K. S. Babu, *Phys. Lett. B* **203**, 132 (1988).
- [73] S. Y. Guo, Z. L. Han, B. Li, Y. Liao and X. D. Ma, *Nucl. Phys. B* **928**, 435 (2018) [arXiv:1707.00522 [hep-ph]].
- [74] T. Nomura, H. Okada and N. Okada, *Phys. Lett. B* **762**, 409 (2016) [arXiv:1608.02694 [hep-ph]].
- [75] K. Cheung, T. Nomura and H. Okada, *Phys. Rev. D* **95**, no. 1, 015026 (2017) [arXiv:1610.04986 [hep-ph]].
- [76] L. M. Krauss, S. Nasri and M. Trodden, *Phys. Rev. D* **67**, 085002 (2003) [hep-ph/0210389].
- [77] R. Foot, H. Lew, X. G. He and G. C. Joshi, *Z. Phys. C* **44**, 441 (1989).
- [78] C. S. Chen, K. L. McDonald and S. Nasri, *Phys. Lett. B* **734**, 388 (2014) [arXiv:1404.6033 [hep-ph]].
- [79] I. Doršner, S. Fajfer, J. F. Kamenik and N. Kosnik, *Phys. Lett. B* **682**, 67 (2009) [arXiv:0906.5585 [hep-ph]].
- [80] C. Hati and U. Sarkar, arXiv:1805.06081 [hep-ph].
- [81] A. Ahriche and S. Nasri, *JCAP* **1307**, 035 (2013) [arXiv:1304.2055 [hep-ph]].
- [82] G. Passarino and M. J. G. Veltman, *Nucl. Phys. B* **160**, 151 (1979).

- [83] J. A. Casas and A. Ibarra, Nucl. Phys. B **618**, 171 (2001) [hep-ph/0103065].
- [84] M. Cirelli, N. Fornengo and A. Strumia, Nucl. Phys. B **753**, 178 (2006) [hep-ph/0512090].
- [85] E. Ma and D. Suematsu, Mod. Phys. Lett. A **24**, 583 (2009) [arXiv:0809.0942 [hep-ph]].
- [86] K. Griest and D. Seckel, Phys. Rev. D **43**, 3191 (1991).
- [87] P. A. R. Ade *et al.* [Planck Collaboration], Astron. Astrophys. **594**, A13 (2016) [arXiv:1502.01589 [astro-ph.CO]].
- [88] S. Choubey, S. Khan, M. Mitra and S. Mondal, Eur. Phys. J. C **78**, no. 4, 302 (2018) [arXiv:1711.08888 [hep-ph]].
- [89] W. Altmannshofer, P. Ball, A. Bharucha, A. J. Buras, D. M. Straub and M. Wick, JHEP **0901**, 019 (2009) [arXiv:0811.1214 [hep-ph]].
- [90] D. Bečirević, N. Košnik, O. Sumensari and R. Zukanovich Funchal, JHEP **1611**, 035 (2016) [arXiv:1608.07583 [hep-ph]].
- [91] G. Hiller and I. Nisandzic, Phys. Rev. D **96**, no. 3, 035003 (2017) [arXiv:1704.05444 [hep-ph]].
- [92] S. Descotes-Genon, L. Hofer, J. Matias and J. Virto, JHEP **1606**, 092 (2016) [arXiv:1510.04239 [hep-ph]].
- [93] T. Hurth, F. Mahmoudi and S. Neshatpour, JHEP **1412**, 053 (2014) [arXiv:1410.4545 [hep-ph]].
- [94] W. Altmannshofer and D. M. Straub, Eur. Phys. J. C **75**, no. 8, 382 (2015) [arXiv:1411.3161 [hep-ph]].
- [95] F. Beaujean, C. Bobeth and D. van Dyk, Eur. Phys. J. C **74**, 2897 (2014) Erratum: [Eur. Phys. J. C **74**, 3179 (2014)] [arXiv:1310.2478 [hep-ph]].
- [96] R. Glattauer *et al.* [Belle Collaboration], Phys. Rev. D **93**, no. 3, 032006 (2016) [arXiv:1510.03657 [hep-ex]].
- [97] A. Abdesselam *et al.* [Belle Collaboration], arXiv:1702.01521 [hep-ex].
- [98] A. J. Buras, D. Buttazzo, J. Girrbach-Noe and R. Knegjens, JHEP **1511**, 033 (2015) [arXiv:1503.02693 [hep-ph]].
- [99] A. V. Artamonov *et al.* [E949 Collaboration], Phys. Rev. Lett. **101**, 191802 (2008) [arXiv:0808.2459 [hep-ex]].
- [100] NA62 Collaboration, Contribution to the "53rd Rencontres de Moriond on Electroweak Interactions and Unified Theories (Moriond EW 2018)", La Thuile, Italy, 10-17 March 2018.
- [101] J. K. Ahn *et al.* [E391a Collaboration], Phys. Rev. D **81**, 072004 (2010) [arXiv:0911.4789 [hep-ex]].
- [102] J. Grygier *et al.* [Belle Collaboration], Phys. Rev. D **96**, no. 9, 091101 (2017) [arXiv:1702.03224 [hep-ex]].
- [103] J. Charles *et al.*, Phys. Rev. D **91**, no. 7, 073007 (2015) [arXiv:1501.05013 [hep-ph]].
- [104] J. Brod and M. Gorbahn, Phys. Rev. Lett. **108**, 121801 (2012) [arXiv:1108.2036 [hep-ph]].
- [105] A. Crivellin, G. D'Ambrosio, M. Hoferichter and L. C. Tunstall, Phys. Rev. D **93**, no. 7, 074038 (2016) [arXiv:1601.00970 [hep-ph]].
- [106] S. Fajfer, N. Košnik and L. Vale Silva, Eur. Phys. J. C **78**, no. 4, 275 (2018) [arXiv:1802.00786 [hep-ph]].
- [107] A. J. Buras, J. Girrbach-Noe, C. Niehoff and D. M. Straub, JHEP **1502**, 184 (2015) [arXiv:1409.4557 [hep-ph]].
- [108] C. Bobeth and A. J. Buras, JHEP **1802**, 101 (2018) [arXiv:1712.01295 [hep-ph]].

- [109] M. Bordone, D. Buttazzo, G. Isidori and J. Monnard, *Eur. Phys. J. C* **77**, no. 9, 618 (2017) [arXiv:1705.10729 [hep-ph]].
- [110] G. Buchalla and A. J. Buras, *Nucl. Phys. B* **400**, 225 (1993).
- [111] M. Misiak and J. Urban, *Phys. Lett. B* **451**, 161 (1999) [hep-ph/9901278].
- [112] G. Buchalla and A. J. Buras, *Nucl. Phys. B* **548**, 309 (1999) [hep-ph/9901288].
- [113] J. Brod, M. Gorbahn and E. Stamou, *Phys. Rev. D* **83**, 034030 (2011) [arXiv:1009.0947 [hep-ph]].
- [114] G. Buchalla and A. J. Buras, *Nucl. Phys. B* **412**, 106 (1994) [hep-ph/9308272].
- [115] A. J. Buras, M. Gorbahn, U. Haisch and U. Nierste, *Phys. Rev. Lett.* **95**, 261805 (2005) [hep-ph/0508165].
- [116] A. J. Buras, M. Gorbahn, U. Haisch and U. Nierste, *JHEP* **0611**, 002 (2006) Erratum: [*JHEP* **1211**, 167 (2012)] [hep-ph/0603079].
- [117] G. Isidori, F. Mescia and C. Smith, *Nucl. Phys. B* **718**, 319 (2005) [hep-ph/0503107].
- [118] A. Lenz *et al.*, *Phys. Rev. D* **83**, 036004 (2011) [arXiv:1008.1593 [hep-ph]].
- [119] M. Bona *et al.* [UTfit Collaboration], *JHEP* **0803**, 049 (2008) [arXiv:0707.0636 [hep-ph]]; New Physics Fit results: Summer 2016, <http://www.utfit.org/UTfit/ResultsSummer2016NP>.
- [120] T. Inami and C. S. Lim, *Prog. Theor. Phys.* **65**, 297 (1981) Erratum: [*Prog. Theor. Phys.* **65**, 1772 (1981)].
- [121] A. J. Buras, hep-ph/9806471.
- [122] A. J. Buras, M. Jamin and P. H. Weisz, *Nucl. Phys. B* **347**, 491 (1990).
- [123] J. Brod and M. Gorbahn, *Phys. Rev. D* **82**, 094026 (2010) [arXiv:1007.0684 [hep-ph]].
- [124] A. J. Buras, *JHEP* **1604**, 071 (2016) [arXiv:1601.00005 [hep-ph]].
- [125] A. J. Buras, F. De Fazio, J. Girrbach and M. V. Carlucci, *JHEP* **1302**, 023 (2013) [arXiv:1211.1237 [hep-ph]].
- [126] A. J. Buras, J. M. Gérard and W. A. Bardeen, *Eur. Phys. J. C* **74**, 2871 (2014) [arXiv:1401.1385 [hep-ph]].
- [127] V. Khachatryan *et al.* [CMS and LHCb Collaborations], *Nature* **522**, 68 (2015) [arXiv:1411.4413 [hep-ex]].
- [128] M. Aaboud *et al.* [ATLAS Collaboration], *Eur. Phys. J. C* **76**, no. 9, 513 (2016) [arXiv:1604.04263 [hep-ex]].
- [129] D. Bečirević, O. Sumensari and R. Zukanovich Funchal, *Eur. Phys. J. C* **76**, no. 3, 134 (2016) [arXiv:1602.00881 [hep-ph]].
- [130] G. D'Ambrosio, G. Isidori and J. Portoles, *Phys. Lett. B* **423**, 385 (1998) [hep-ph/9708326].
- [131] A. M. Baldini *et al.* [MEG Collaboration], *Eur. Phys. J. C* **76**, no. 8, 434 (2016) [arXiv:1605.05081 [hep-ex]].
- [132] A. M. Baldini *et al.* [MEG II Collaboration], *Eur. Phys. J. C* **78**, no. 5, 380 (2018) [arXiv:1801.04688 [physics.ins-det]].
- [133] G. Cavoto, A. Papa, F. Renga, E. Ripicini and C. Voena, *Eur. Phys. J. C* **78**, no. 1, 37 (2018) [arXiv:1707.01805 [hep-ex]].
- [134] B. Aubert *et al.* [BaBar Collaboration], *Phys. Rev. Lett.* **104**, 021802 (2010) [arXiv:0908.2381 [hep-ex]].
- [135] T. Aushev *et al.*, arXiv:1002.5012 [hep-ex].

- [136] U. Bellgardt *et al.* [SINDRUM Collaboration], Nucl. Phys. B **299**, 1 (1988).
- [137] A. Blondel *et al.*, arXiv:1301.6113 [physics.ins-det].
- [138] K. Hayasaka *et al.*, Phys. Lett. B **687**, 139 (2010) [arXiv:1001.3221 [hep-ex]].
- [139] W. H. Bertl *et al.* [SINDRUM II Collaboration], Eur. Phys. J. C **47**, 337 (2006).
- [140] T. M. Nguyen [DeeMe Collaboration], PoS FPCP **2015**, 060 (2015).
- [141] B. E. Krikler [COMET Collaboration], arXiv:1512.08564 [physics.ins-det].
- [142] L. Bartoszek *et al.* [Mu2e Collaboration], arXiv:1501.05241 [physics.ins-det].
- [143] Y. Kuno, Nucl. Phys. Proc. Suppl. **149**, 376 (2005).
- [144] I. Doršner, S. Fajfer, A. Greljo, J. F. Kamenik and N. Košnik, Phys. Rept. **641**, 1 (2016) [arXiv:1603.04993 [hep-ph]].
- [145] Y. Kuno and Y. Okada, Rev. Mod. Phys. **73**, 151 (2001) [hep-ph/9909265].
- [146] Y. Okada, K. i. Okumura and Y. Shimizu, Phys. Rev. D **61**, 094001 (2000) [hep-ph/9906446].
- [147] S. Davidson, Y. Kuno and A. Saporta, Eur. Phys. J. C **78**, no. 2, 109 (2018) [arXiv:1710.06787 [hep-ph]].
- [148] R. Kitano, M. Koike and Y. Okada, Phys. Rev. D **66**, 096002 (2002) Erratum: [Phys. Rev. D **76**, 059902 (2007)] [hep-ph/0203110].
- [149] M. Aaboud *et al.* [ATLAS Collaboration], New J. Phys. **18**, no. 9, 093016 (2016) [arXiv:1605.06035 [hep-ex]].
- [150] A. M. Sirunyan *et al.* [CMS Collaboration], JHEP **1707**, 121 (2017) [arXiv:1703.03995 [hep-ex]].
- [151] The ATLAS collaboration [ATLAS Collaboration], ATLAS-CONF-2016-078.
- [152] M. Aaboud *et al.* [ATLAS Collaboration], Eur. Phys. J. C **76**, no. 10, 547 (2016) [arXiv:1606.08772 [hep-ex]].
- [153] C. D. Froggatt and H. B. Nielsen, Nucl. Phys. B **147**, 277 (1979).
- [154] A. E. Cárcamo Hernández, I. de Medeiros Varzielas and E. Schumacher, arXiv:1601.00661 [hep-ph].
- [155] A. E. Cárcamo Hernández, I. de Medeiros Varzielas and E. Schumacher, Phys. Rev. D **93**, no. 1, 016003 (2016) [arXiv:1509.02083 [hep-ph]].
- [156] A. E. Cárcamo Hernández, Eur. Phys. J. C **76**, no. 9, 503 (2016) [arXiv:1512.09092 [hep-ph]].
- [157] M. D. Campos, A. E. Cárcamo Hernández, H. Päs and E. Schumacher, Phys. Rev. D **91**, no. 11, 116011 (2015) [arXiv:1408.1652 [hep-ph]].
- [158] R. Barbieri, G. Isidori, A. Pattori and F. Senia, Eur. Phys. J. C **76**, no. 2, 67 (2016) [arXiv:1512.01560 [hep-ph]].
- [159] R. Alonso, M. Dhen, M. B. Gavela and T. Hambye, JHEP **1301**, 118 (2013) [arXiv:1209.2679 [hep-ph]].
- [160] P. F. de Salas, D. V. Forero, C. A. Ternes, M. Tortola and J. W. F. Valle, Phys. Lett. B **782**, 633 (2018) [arXiv:1708.01186 [hep-ph]].